PHYSICAL REVIEW D **94,** 014501 (2016)

Spectral properties and chiral symmetry violations of (staggered) domain wall fermions in the Schwinger model

Christian Hoelbling
Department of Physics, Wuppertal University, D-42119 Wuppertal, Germany

Christian Zielinski
Division of Mathematical Sciences, Nanyang Technological University, Singapore 637371, Singapore and Department of Physics, Wuppertal University, D-42119 Wuppertal, Germany

(Received 8 March 2016; revised manuscript received 25 May 2016; published 5 July 2016)

We follow up on a suggestion by Adams and construct explicit domain wall fermion operators with staggered kernels. We compare different domain wall formulations, namely the standard construction as well as Boriçi's modified and Chiu's optimal construction, utilizing both Wilson and staggered kernels. In the process, we generalize the staggered kernels to arbitrary even dimensions and introduce both truncated and optimal staggered domain wall fermions. Some numerical investigations are carried out in the $(1+1)$-dimensional setting of the Schwinger model, where we explore spectral properties of the bulk, effective and overlap Dirac operators in the free-field case, on quenched thermalized gauge configurations and on smooth topological configurations. We compare different formulations using the effective mass, deviations from normality and violations of the Ginsparg-Wilson relation as measures of chirality.

DOI: 10.1103/PhysRevD.94.014501

I. INTRODUCTION

Chiral symmetry plays a crucial role in the understanding of hadron phenomenology and the low-energy dynamics of quantum chromodynamics (QCD). On the lattice, the overlap construction [1–7] allows one to implement a fermion operator with exact chiral symmetry [8–10], thus evading the Nielsen-Ninomiya theorem [11–14]. In practice, the use of overlap fermions is limited by the fact that they generically require a factor of $\mathcal{O}(10\text{–}100)$ more computational resources than Wilson fermions, and tunneling between topological sectors is severely suppressed even at moderate lattice spacings [15–18].

Domain wall fermions [19–21] offer an alternative by formulating fermions with approximate chiral symmetry in d dimensions by means of massive interacting fermions in $d+1$ dimensions ($d=2,\ 4$). The limit of an infinite extension of the extra dimension can again be expressed as an overlap operator with exact chiral symmetry. For a finite extent, domain wall fermions can then be seen as a truncation of overlap fermions. They offer the possibility of reducing computational cost and are well suited for parallel implementations. This comes at the price of replacing the exact chiral symmetry by an approximate one. It is expected that chiral symmetry violations are exponentially suppressed [20,22–24], although in practice this suppression can still require large extents of the extra dimension [25–29]. However, these violations also facilitate the tunneling between topological sectors.

Domain wall fermions are typically formulated with a Wilson kernel [30]. Only recently has it been clarified by Adams [31,32] how to utilize the computationally more efficient staggered fermions [33–36] in its place by giving staggered fermions a flavor-dependent mass; see also Refs. [37–39]. Subsequent numerical work [40–43] focused on the properties of these staggered Wilson fermions and their use as a kernel for an overlap construction [32]. The possibility of staggered domain wall fermions, which was also suggested in Ref. [32], has however not been investigated any further. The present work is meant as a first step in closing this gap. We give explicit constructions of staggered domain wall fermions and compare their spectral and chiral symmetry breaking properties to those of traditional domain wall fermions with Wilson fermions in the context of the Schwinger model [44].

While we are eventually interested in QCD, the Schwinger model, i.e. $(1+1)$-dimensional quantum electrodynamics (QED), retains enough properties of QCD. In particular, we find confinement and topological structure, making it useful for conceptual investigations. On the other hand, it is numerically simple enough to allow the computation of the complete eigenvalue spectrum of fermion operators on nontrivial background configurations. Moreover, the study of fermions in $1+1$ dimensions naturally arises e.g. in the low-energy description of conducting electrons in metals, see Ref. [45].

This paper is organized as follows. In Sec. II, we discuss the kernel operators, among them generalizations of staggered Wilson fermions in an arbitrary even number of dimensions. In Sec. III, the construction of (staggered) domain wall fermions and their variations are given, in Sec. IV we introduce the effective Dirac operators and

discuss the limiting overlap operators, in Sec. V we explain our approach of carrying out the numerical calculations and in Sec. VI we discuss the numerical results. In Sec. VII, we conclude our work and give an outlook.

II. KERNEL OPERATORS

We begin by giving a quick review of the kernel operators we are considering, namely Wilson and staggered Wilson fermions. Here and in the following, we are mostly interested in the $(1+1)$-dimensional case ($d=2$), but where convenient we write down the general d-dimensional expressions.

A. Wilson kernel

For Wilson fermions [46], the Dirac operator reads

$$D_{\mathsf{w}}(m_{\mathsf{f}}) = \gamma_\mu \nabla_\mu + m_{\mathsf{f}} + W_{\mathsf{w}}. \tag{1}$$

Here the γ_μ matrices refer to a representation of the Dirac algebra $\{\gamma_\mu, \gamma_\nu\} = 2\delta_{\mu,\nu}\mathbb{1}$ with $\mu \in \{1, \ldots, d\}$, $\delta_{\mu,\nu}$ to the Kronecker delta, ∇_μ to the covariant central finite difference operator and m_{f} to the bare fermion mass. The Wilson term reads

$$W_{\mathsf{w}} = -\frac{ar}{2}\Delta \tag{2}$$

with lattice spacing a, Wilson parameter $r \in (0, 1]$ and the covariant lattice Laplacian Δ. We note that $D_{\mathsf{w}}^\dagger = \gamma_{d+1} D_{\mathsf{w}} \gamma_{d+1}$, where γ_{d+1} is the chirality matrix, and that the W_{w} term breaks chiral symmetry explicitly. In terms of the parallel transport

$$T_\mu \Psi(x) = U_\mu(x)\Psi(x + a\hat{\mu}), \tag{3}$$

we have the following definitions:

$$\nabla_\mu = \frac{1}{2a}(T_\mu - T_\mu^\dagger), \tag{4}$$

$$C_\mu = \frac{1}{2}(T_\mu + T_\mu^\dagger), \tag{5}$$

$$\Delta = \frac{2}{a^2}\sum_\mu (C_\mu - \mathbb{1}). \tag{6}$$

Through the Wilson term W_{w}, the doublers acquire a mass $\mathcal{O}(a^{-1})$. In the continuum limit, the number of flavors is then reduced from 2^d to one physical flavor.

B. Staggered Wilson fermions

Following Refs. [31,32,37,38,41,42], in $d=4$ dimensions a staggered Wilson operator can be written as

$$D_{\mathsf{sw}}(m_{\mathsf{f}}) = D_{\mathsf{st}} + m_{\mathsf{f}} + W_{\mathsf{st}} \tag{7}$$

with staggered Dirac operator

$$D_{\mathsf{st}} = \eta_\mu \nabla_\mu, \tag{8}$$

$$\eta_\mu \chi(x) = (-1)^{\sum_{\nu<\mu} x_\nu/a}\chi(x) \tag{9}$$

and bare fermion mass m_{f}. The staggered Wilson term is an operator that, up to discretization terms, is trivial in spin but splits the different flavors. We also require the Dirac operator to have a real determinant. The original suggestion by Adams [31,32] reads

$$W_{\mathsf{st}} = \frac{r}{a}(\mathbb{1} + \Gamma_{1234} C_{1234}) \tag{10}$$

with a Wilson-like parameter $r > 0$ and operators

$$\Gamma_{1234}\chi(x) = (-1)^{\sum_\mu x_\mu/a}\chi(x), \tag{11}$$

$$C_{1234} = \eta_1\eta_2\eta_3\eta_4 (C_1 C_2 C_3 C_4)_{\mathsf{sym}}. \tag{12}$$

In the spin-flavor basis, this term has the form

$$W_{\mathsf{st}} \sim \frac{r}{a}\mathbb{1} \otimes (\mathbb{1} - \xi_5) + \mathcal{O}(a), \tag{13}$$

which splits the four flavors into pairs of two according to their "flavor chirality", i.e. the eigenbasis of ξ_5. The notation $A \sim B$ means that B corresponds to the respective spin $\otimes$ flavor interpretation [37] of A up to proportionality, while the ξ_μ are a representation of the Dirac algebra in flavor space. The determinant of D_{sw} is real due to the ϵ-Hermiticity

$$D_{\mathsf{sw}}^\dagger = \epsilon D_{\mathsf{sw}} \epsilon \tag{14}$$

with

$$\epsilon(x) = (-1)^{\sum_\mu x_\mu/a}. \tag{15}$$

In four dimensions, one may also split the flavors with respect to the eigenbasis of different elements of the flavor Dirac algebra [37,38]. To retain ϵ Hermiticity and, thus, a real determinant, the flavor structure of the mass term needs to be restricted to a sum of products of an even number of ξ_μ. A single flavor staggered fermion in four dimensions can, thus, be obtained by e.g.

$$W_{\mathsf{st}} = \frac{r}{a}(2\cdot\mathbb{1} + W_{\mathsf{st}}^{12} + W_{\mathsf{st}}^{34}), \tag{16}$$

$$W_{\mathsf{st}}^{\mu\nu} = \mathrm{i}\Gamma_{\mu\nu} C_{\mu\nu}, \tag{17}$$

where the operators $\Gamma_{\mu\nu}$ and $C_{\mu\nu}$ are given by

$$\Gamma_{\mu\nu}\chi(x) = \varepsilon_{\mu\nu}(-1)^{(x_\mu+x_\nu)/a}\chi(x), \tag{18}$$

$$C_{\mu\nu} = \eta_\mu\eta_\nu \cdot \frac{1}{2}(C_\mu C_\nu + C_\nu C_\mu) \quad \text{(no sum)}. \tag{19}$$

Here and in the following, $\varepsilon_{\mu_1\cdots\mu_N}$ refers to the Levi-Civita symbol. To interpret the mass term in Eq. (17), note that

$$\Gamma_{\mu\nu} \sim \gamma_\mu\gamma_\nu \otimes \xi_\mu\xi_\nu, \tag{20}$$

$$C_{\mu\nu} \sim \gamma_\mu\gamma_\nu \otimes \mathbb{1}, \tag{21}$$

$$\epsilon \sim \gamma_5 \otimes \xi_5, \tag{22}$$

up to discretization terms. As a result, we find for the staggered Wilson term

$$W_{\text{st}}^{\mu\nu} \sim \mathbb{1} \otimes \sigma_{\mu\nu} + \mathcal{O}(a) \tag{23}$$

with $\sigma_{\mu\nu} = \mathrm{i}\xi_\mu\xi_\nu$. This implies that the number of physical fermion species of W_{st} is reduced to one by giving all but a single flavor a mass $\mathcal{O}(a^{-1})$.

These results can be formulated in an arbitrary even number of dimensions d, where we can write a single flavor mass term as

$$W_{\text{st}} = \frac{r}{a}\sum_{k=1}^{d/2}(\mathbb{1} + W_{\text{st}}^{(2k-1)(2k)}) \tag{24}$$

and Eq. (16) now follows as the special case $d = 4$. To construct a more general mass term, we define

$$W_{\text{st}}^{\mu_1\cdots\mu_{2n}} = \mathrm{i}^n\Gamma_{\mu_1\cdots\mu_{2n}}C_{\mu_1\cdots\mu_{2n}}, \tag{25}$$

for an arbitrary $n \le d/2$, where

$$\Gamma_{\mu_1\cdots\mu_{2n}}\chi(x) = \varepsilon_{\mu_1\cdots\mu_{2n}}(-1)^{\sum_{i=1}^{2n}x_{\mu_i}/a}\chi(x), \tag{26}$$

$$C_{\mu_1\cdots\mu_{2n}} = \eta_{\mu_1}\cdots\eta_{\mu_{2n}}(C_{\mu_1}\cdots C_{\mu_{2n}})_{\text{sym}}. \tag{27}$$

In the spin $\otimes$ flavor interpretation, we find

$$\Gamma_{\mu_1\cdots\mu_{2n}} \sim (\gamma_{\mu_1}\ldots\gamma_{\mu_{2n}}) \otimes (\xi_{\mu_1}\ldots\xi_{\mu_{2n}}), \tag{28}$$

$$C_{\mu_1\cdots\mu_{2n}} \sim (\gamma_{\mu_1}\ldots\gamma_{\mu_{2n}}) \otimes \mathbb{1}, \tag{29}$$

$$W_{\text{st}}^{\mu_1\cdots\mu_{2n}} \sim \mathbb{1} \otimes (\mathrm{i}^n\xi_{\mu_1}\ldots\xi_{\mu_{2n}}), \tag{30}$$

up to discretization terms. In addition, the new mass terms fulfill the ϵ-Hermiticity relation

$$W^\dagger = \epsilon W \epsilon, \qquad W \equiv W_{\text{st}}^{\mu_1\cdots\mu_{2n}}. \tag{31}$$

We can, thus, replace Eq. (24) by a generic

$$W_{\text{st}} = \sum_{n=1}^{d/2}\sum_{\boldsymbol{\mu}_n}\frac{r_{\boldsymbol{\mu}_n}}{a}(\mathbb{1} + W_{\text{st}}^{\boldsymbol{\mu}_n}), \tag{32}$$

where $r_{\boldsymbol{\mu}_n} \ge 0$ and the sum is over all multi-indices $\boldsymbol{\mu}_n = (\mu_1, \ldots, \mu_{2n})$ with $1 \le \mu_i \le d$ for all i with $1 \le i \le 2n$ [47]. Adams' original mass term in $d = 4$ dimensions in Eq. (10) then follows from setting $r_{1234} = r > 0$ and $r_{\boldsymbol{\mu}_n} = 0$ otherwise.

For the $d = 2$ case that we will consider in the numerical part of this paper, the definition is essentially unique and reads

$$W_{\text{st}} = \frac{r}{a}(\mathbb{1} + W_{\text{st}}^{12}). \tag{33}$$

In this case, the reduction is from two staggered flavors to a single physical one.

Like in the Wilson case, all possible W_{st} terms break chiral symmetry explicitly. Furthermore, there may be additional counterterms if too many of the staggered symmetries are broken [39].

III. DOMAIN WALL FERMIONS

After having introduced the kernel operators, we now move on to the domain wall fermion Dirac operators. Originally proposed by Kaplan [19], then refined by Shamir and Furman [20,21], the domain wall construction implements approximately massless fermions in d dimensions by means of a $(d+1)$-dimensional theory. Equivalently, domain wall fermions can be understood as a tower of N_s fermions in d dimensions with a particular flavor structure.

We now give a quick summary of the well-known $(d+1)$-dimensional formulations. For the remainder of the paper we fix the d-dimensional lattice spacing to $a = 1$ and the (staggered) Wilson parameter to $r = 1$.

A. Standard construction

We begin with the standard construction. First, let us define

$$D_{\text{w}}^{\pm} = a_{d+1}D_{\text{w}}(-M_0) \pm \mathbb{1}, \tag{34}$$

where we explicitly write out the lattice spacing a_{d+1} in the extra dimension. The parameter M_0 is the so-called domain wall height and must be suitably chosen for the description of a single flavor. In the free-field case, we have $M_0 \in (0, 2r)$.

The Dirac operator reads

$$\overline{\Psi}D_{\text{dw}}\Psi = \sum_{s=1}^{N_s}\overline{\Psi}_s[D_{\text{w}}^{+}\Psi_s - P_-\Psi_{s+1} - P_+\Psi_{s-1}] \tag{35}$$

with $(d+1)$-dimensional fermion fields $\overline{\Psi}$, Ψ and chiral projectors $P_\pm = \frac{1}{2}(\mathbb{1} \pm \gamma_{d+1})$. Here and in the following, the index s refers to the additional spatial (or equivalently flavor) coordinate. The gauge links are taken to be the identity matrix along the additional coordinate. Furthermore, we impose the following boundary conditions,

$$P_+(\Psi_0 + m\Psi_{N_s}) = 0, \tag{36}$$

$$P_-(\Psi_{N_s+1} + m\Psi_1) = 0, \tag{37}$$

where m is related to the bare fermion mass, see Eq. (76). We note that in the special case of $m = 0$ we find Dirichlet boundary conditions in the extra dimension, while for $m = \pm 1$ one recovers (anti-)periodic boundary conditions. If we write down the Dirac operator in the extra dimension explicitly, we find

$$D_{\mathsf{dw}} = \begin{pmatrix} D_{\mathsf{w}}^+ & -P_- & & & mP_+ \\ -P_+ & D_{\mathsf{w}}^+ & -P_- & & \\ & \ddots & \ddots & \ddots & \\ & & -P_+ & D_{\mathsf{w}}^+ & -P_- \\ mP_- & & & -P_+ & D_{\mathsf{w}}^+ \end{pmatrix}. \tag{38}$$

One possibility of constructing the d-dimensional fermion fields from the boundary is via

$$q = P_+\Psi_{N_s} + P_-\Psi_1, \qquad \overline{q} = \overline{\Psi}_1 P_+ + \overline{\Psi}_{N_s} P_-. \tag{39}$$

Let us also define the reflection operator along the extra dimension

$$R = \begin{pmatrix} & & \mathbb{1} \\ & \iddots & \\ \mathbb{1} & & \end{pmatrix}. \tag{40}$$

We find that D_{dw} is $R\gamma_{d+1}$-Hermitian

$$D_{\mathsf{dw}}^\dagger = R\gamma_{d+1} \cdot D_{\mathsf{dw}} \cdot R\gamma_{d+1}, \tag{41}$$

which ensures that $\det D_{\mathsf{dw}} \in \mathbb{R}$ and the applicability of importance sampling techniques.

Besides this canonical formulation, several variations of domain wall fermions have been proposed.

B. Boriçi's construction

One of them is the construction by Boriçi [48], which follows from the original proposal by the replacements

$$P_+\Psi_{s-1} \to -D_{\mathsf{w}}^- P_+ \Psi_{s-1}, \tag{42}$$

$$P_-\Psi_{s+1} \to -D_{\mathsf{w}}^- P_- \Psi_{s+1}. \tag{43}$$

Note that this is an $\mathcal{O}(a_{d+1})$ modification. The Dirac operator in its full form reads

$$\overline{\Psi} D_{\mathsf{dw}} \Psi = \sum_{s=1}^{N_s} \overline{\Psi}_s [D_{\mathsf{w}}^+ \Psi_s + D_{\mathsf{w}}^- P_- \Psi_{s+1} + D_{\mathsf{w}}^- P_+ \Psi_{s-1}] \tag{44}$$

or explicitly

$$D_{\mathsf{dw}} = \begin{pmatrix} D_{\mathsf{w}}^+ & D_{\mathsf{w}}^- P_- & & & -mD_{\mathsf{w}}^- P_+ \\ D_{\mathsf{w}}^- P_+ & D_{\mathsf{w}}^+ & D_{\mathsf{w}}^- P_- & & \\ & \ddots & \ddots & \ddots & \\ & & D_{\mathsf{w}}^- P_+ & D_{\mathsf{w}}^+ & D_{\mathsf{w}}^- P_- \\ -mD_{\mathsf{w}}^- P_- & & & D_{\mathsf{w}}^- P_+ & D_{\mathsf{w}}^+ \end{pmatrix}. \tag{45}$$

Furthermore, Eq. (39) generalizes to

$$q = P_+\Psi_{N_s} + P_-\Psi_1, \tag{46}$$

$$\overline{q} = -\overline{\Psi}_1 D_{\mathsf{w}}^- P_+ - \overline{\Psi}_{N_s} D_{\mathsf{w}}^- P_-, \tag{47}$$

and Eq. (41) to

$$(\mathcal{D}^{-1} D_{\mathsf{dw}})^\dagger = R\gamma_{d+1} \cdot (\mathcal{D}^{-1} D_{\mathsf{dw}}) \cdot R\gamma_{d+1}, \tag{48}$$

$$\mathcal{D} = \mathbb{1}_{N_s} \otimes D_{\mathsf{w}}^- \tag{49}$$

(see Ref. [49]). This formulation is also known as "truncated overlap fermions" as the corresponding d-dimensional effective operator equals the polar decomposition approximation [6,50] of order $N_s/2$ of Neuberger's overlap operator (for even N_s).

C. Optimal construction

The last modification we consider are the optimal domain wall fermions proposed by Chiu [51,52]. The idea is to modify D_{dw} in such a way, that the effective Dirac operator is expressed through Zolotarev's optimal rational approximation of the sign function [53–55] (see also Refs. [56,57]). In the following, we quote the central formulas of the construction given in Ref. [51].

Starting from Boriçi's construction, the Dirac operator is modified by introducing weight factors

$$\overline{\Psi} D_{\mathsf{dw}} \Psi = \sum_{s=1}^{N_s} \overline{\Psi}_s D_{\mathsf{w}}^{+}(s) \Psi_s + \sum_{s=1}^{N_s} \overline{\Psi}_s [D_{\mathsf{w}}^{-}(s) P_{-} \Psi_{s+1} + D_{\mathsf{w}}^{-}(s) P_{+} \Psi_{s-1}], \tag{50}$$

where

$$D_{\mathsf{w}}^{\pm}(s) = a_{d+1} \omega_s D_{\mathsf{w}}(-M_0) \pm \mathbb{1}. \tag{51}$$

The weight factors ω_s are given by

$$\omega_s = \frac{1}{\lambda_{\mathsf{min}}} \sqrt{1 - \kappa'^2 \mathrm{sn}(v_s, \kappa')} \tag{52}$$

with $\mathrm{sn}(v_s, \kappa')$ being the corresponding Jacobi elliptic function with argument v_s and modulus κ'. The modulus is defined by

$$\kappa' = \sqrt{1 - \lambda_{\mathsf{min}}^2 / \lambda_{\mathsf{max}\,ax}^2} \tag{53}$$

and λ_{min}^2 (λ_{max}^2) is the respective smallest (largest) eigenvalue of H_{w}^2 with

$$H_{\mathsf{w}} = \gamma_{d+1} D_{\mathsf{w}}(-M_0). \tag{54}$$

The argument v_s reads

$$v_s = (-1)^{s-1} M \mathrm{sn}^{-1}\left(\sqrt{\frac{1+3\lambda}{(1+\lambda)^3}}, \sqrt{1-\lambda^2} \right) + \left\lfloor \frac{s}{2} \right\rfloor \frac{2K'}{N_s}, \tag{55}$$

where

$$\lambda = \prod_{\ell=1}^{N_s} \frac{\Theta^2(2\ell K'/N_s, \kappa')}{\Theta^2((2\ell-1)K'/N_s, \kappa')}, \tag{56}$$

$$M = \prod_{\ell=1}^{\lfloor N_s/2 \rfloor} \frac{\mathrm{sn}^2((2\ell-1)K'/N_s, \kappa')}{\mathrm{sn}^2(2\ell K'/N_s, \kappa')}. \tag{57}$$

Here $\lfloor \cdot \rfloor$ refers to the floor function, $K' = K(\kappa')$ to the complete elliptic integral of the first kind with

$$K(k) = \int_0^{\pi/2} \frac{\mathrm{d}\theta}{\sqrt{1 - k^2 \sin^2\theta}}. \tag{58}$$

Furthermore we introduced the elliptic Theta function via

$$\Theta(w, k) = \vartheta_4\left(\frac{\pi w}{2K}, k \right) \tag{59}$$

with $K = K(k)$ and elliptic theta functions ϑ_i [58]. Some reference values for the weight factors $\{\omega_s\}$ can be found in Appendix A.

Similarly to Boriçi's construction, Eq. (39) now generalizes to

$$q = P_{+} \Psi_{N_s} + P_{-} \Psi_1, \tag{60}$$

$$\overline{q} = -\overline{\Psi}_1 D_{\mathsf{w}}^{-}(1) P_{+} - \overline{\Psi}_{N_s} D_{\mathsf{w}}^{-}(N_s) P_{-} \tag{61}$$

and Eq. (41) again to Eq. (48), but now with

$$\mathcal{D} = \mathrm{diag}[D_{\mathsf{w}}^{-}(1), \ldots, D_{\mathsf{w}}^{-}(N_s)], \tag{62}$$

as pointed out in Ref. [49]. Optimal domain wall fermions have been and are still extensively used. Some of the results obtained can be found in Refs. [59–64].

We also note that there is a modified construction of optimal domain wall fermions [65], which is reflection-symmetric along the fifth dimension. For completeness we point out that all the preceding domain wall fermion formulations can be seen as special cases of Möbius domain wall fermions [49,66,67].

D. Staggered formulations

As proposed in Ref. [32], we can use the staggered Wilson kernel to formulate a staggered version of domain wall fermions. We can write the Dirac operator in a general d-dimensional form as

$$\overline{\Upsilon} D_{\mathsf{sdw}} \Upsilon = \sum_{s=1}^{N_s} \overline{\Upsilon}_s [D_{\mathsf{sw}}^{+} \Upsilon_s - P_{-} \Upsilon_{s+1} - P_{+} \Upsilon_{s-1}], \tag{63}$$

where Υ refers to the staggered fermion field. Like in the Wilson case we define

$$D_{\mathsf{sw}}^{\pm} = a_{d+1} D_{\mathsf{sw}}(-M_0) \pm \mathbb{1}. \tag{64}$$

The chiral projectors are given by $P_{\pm} = \frac{1}{2}(\mathbb{1} \pm \epsilon)$, where $\epsilon^2 = \mathbb{1}$. Here we have $\epsilon \sim \gamma_{d+1} \otimes \xi_{d+1}$, which reduces to $\epsilon \sim \gamma_{d+1} \otimes \mathbb{1}$ on the physical species. One can easily verify the $R\epsilon$-Hermiticity of D_{sdw}. Note that we follow a sign convention in where our D_{sdw} is in full analogy to D_{dw}, while in Ref. [32] a slightly different convention is used. The staggered domain wall Dirac operator D_{sdw} can be constructed from D_{dw} by the replacement rule given in Ref. [32], which we write down in a general d-dimensional form as

$$\gamma_{d+1} \to \epsilon, \qquad D_{\mathsf{w}} \to D_{\mathsf{sw}}. \tag{65}$$

Using the replacement rule in Eq. (65), we can also generalize Boriçi's and the optimal construction to the case of a staggered Wilson kernel. This gives rise to previously

not considered truncated staggered domain wall fermions with the Dirac operator

$$\overline{\Upsilon} D_{\mathsf{sdw}} \Upsilon = \sum_{s=1}^{N_s} \overline{\Upsilon}_s D_{\mathsf{sw}}^{+} \Upsilon_s + \sum_{s=1}^{N_s} \overline{\Upsilon}_s [D_{\mathsf{sw}}^{-} P_{-} \Upsilon_{s+1} + D_{\mathsf{sw}}^{-} P_{+} \Upsilon_{s-1}] \tag{66}$$

as well as optimal staggered domain wall fermions

$$\overline{\Upsilon} D_{\mathsf{sdw}} \Upsilon = \sum_{s=1}^{N_s} \overline{\Upsilon}_s D_{\mathsf{sw}}^{+}(s) \Upsilon_s + \sum_{s=1}^{N_s} \overline{\Upsilon}_s [D_{\mathsf{sw}}^{-}(s) P_{-} \Upsilon_{s+1} + D_{\mathsf{sw}}^{-}(s) P_{+} \Upsilon_{s-1}], \tag{67}$$

where $D_{\mathsf{sw}}^{\pm}(s) = a_{d+1}\omega_s D_{\mathsf{sw}}(-M_0) \pm \mathbb{1}$ and the weight factors ω_s are given by Eq. (52) for the kernel $H_{\mathsf{sw}} = \epsilon D_{\mathsf{sw}}(-M_0)$.

IV. EFFECTIVE DIRAC OPERATOR

To understand the relation between the $(d+1)$-dimensional fermions and the light d-dimensional fields q, $\overline{q}$ at the boundary, we introduce the effective d-dimensional Dirac operator as derived in Refs. [48,68–70] (see also Refs. [71,72]). In the following, we give a short summary, following Refs. [48,69,72].

A. Derivation

The low energy effective d-dimensional action

$$S_{\mathsf{eff}} = \sum_x \overline{q}(x) D_{\mathsf{eff}} q(x) \tag{68}$$

follows after integrating out the $N_s - 1$ heavy modes. The effective Dirac operator is defined via the propagator

$$D_{\mathsf{eff}}^{-1}(x,y) = \langle q(x)\overline{q}(y)\rangle. \tag{69}$$

For a suitable choice of M_0, there is exactly one light and $N_s - 1$ heavy Dirac fermions.

In the chiral limit $N_s \to \infty$ (at fixed bare coupling β), the contribution from the heavy fermions diverges. This bulk contribution from the $(d+1)$-dimensional fermions can be canceled by the introduction of suitable pseudofermion fields. One typically chooses the fermion action with the replacement $m \to 1$ as the action for the pseudofermions.

Let us begin by defining the Hermitian operators

$$H_{\mathsf{w}} = \gamma_{d+1} D_{\mathsf{w}}(-M_0), \tag{70}$$

$$H_{\mathsf{m}} = \gamma_{d+1} D_{\mathsf{m}}(-M_0), \tag{71}$$

where the kernel operator of standard domain wall fermions is given by

$$D_{\mathsf{m}}(-M_0) = \frac{D_{\mathsf{w}}(-M_0)}{2\cdot\mathbb{1} + a_{d+1} D_{\mathsf{w}}(-M_0)}. \tag{72}$$

The transfer matrix along the extra dimension is given by

$$T = \frac{T_-}{T_+}, \qquad T_\pm = \mathbb{1} \pm a_{d+1} H, \tag{73}$$

where we use the notation

$$H = \begin{cases} H_{\mathsf{m}} & \text{for standard constr.,} \\ H_{\mathsf{w}} & \text{for Boriçi's constr.} \end{cases} \tag{74}$$

Then the effective operator can be written as

$$D_{\mathsf{eff}} = \frac{1+m}{2}\mathbb{1} + \frac{1-m}{2}\gamma_{d+1}\frac{T_+^{N_s} - T_-^{N_s}}{T_+^{N_s} + T_-^{N_s}}. \tag{75}$$

Note that we can rewrite Eq. (75) as

$$D_{\mathsf{eff}} = (1-m)\left[D_{\mathsf{eff}}(0) + \frac{m}{1-m}\right], \tag{76}$$

where $D_{\mathsf{eff}}(0)$ denotes the effective operator D_{eff} at $m = 0$. We can see that the parameter m induces a bare fermion mass of $m/(1-m)$, see Ref. [73].

Alternatively, one can also show [48,72] the relation

$$D_{\mathsf{eff}} = (\mathcal{P}^{\intercal} D_1^{-1} D_m \mathcal{P})_{1,1} \tag{77}$$

with the matrix $\mathcal{P}$ defined as

$$\mathcal{P} = \begin{pmatrix} P_- & P_+ & & & \\ & P_- & P_+ & & \\ & & \ddots & \ddots & \\ & & & P_- & P_+ \\ P_+ & & & & P_- \end{pmatrix} \tag{78}$$

and $\mathcal{P}^{-1} = \mathcal{P}^{\intercal}$. Here we used the shorthand notation $D_m = D_{\mathsf{dw}}(m)$, while the index stands for the (1,1) s-block of the matrix.

The derivation of the effective operator for optimal domain wall fermions follows Boriçi's construction after including the weight factors $\{\omega_s\}$ appropriately [51]. By construction the sign-function approximation equals the optimal rational approximation. It can be either evaluated directly or via the projection method of Eq. (77).

B. The $N_s \to \infty$ limit

In the following, let us specialize to $m = 0$. Note that we can rewrite Eq. (75) using

$$\frac{T_+^{N_s} - T_-^{N_s}}{T_+^{N_s} + T_-^{N_s}} = \epsilon_{N_s/2}(a_{d+1}H), \tag{79}$$

where $\epsilon_{N_s/2}$ is Neuberger's polar decomposition approximation [6,50] of the sign-function. Therefore, we obtain an overlap operator in the $N_s \to \infty$ limit as follows,

$$\begin{aligned} D_{\mathrm{ov}} &= \lim_{N_s\to\infty} D_{\mathrm{eff}} \\ &= \frac{1}{2}\mathbb{1} + \frac{1}{2}\gamma_{d+1}\mathrm{sign}\, H \\ &= \frac{1}{2}[\mathbb{1} + D_{-M_0}(D_{-M_0}^\dagger D_{-M_0})^{-\frac{1}{2}}], \end{aligned} \tag{80}$$

with H given in Eq. (74), $D_{-M_0} = D(-M_0)$ and

$$D = \begin{cases} D_{\mathrm{m}} & \text{for standard constr.,} \\ D_{\mathrm{w}} & \text{for Boriçi's/Chiu's constr.} \end{cases} \tag{81}$$

The overlap operator satisfies the Ginsparg-Wilson equation

$$\{\gamma_{d+1}, D_{\mathrm{ov}}\} = 2D_{\mathrm{ov}}\gamma_{d+1}D_{\mathrm{ov}} \tag{82}$$

and allows for an exact chiral symmetry. Eq. (82) also implies the normality of the overlap operator as can be easily verified.

Comparing Eq. (80) to the standard definition of the overlap operator

$$D_{\mathrm{ov}} = \rho[\mathbb{1} + D_{-\rho}(D_{-\rho}^\dagger D_{-\rho})^{-\frac{1}{2}}] \tag{83}$$

and using the relation for the effective negative mass parameter

$$\rho = \begin{cases} M_0 - \frac{a_{d+1}}{2}M_0^2 & \text{for standard constr.,} \\ M_0 & \text{for Boriçi's/Chiu's constr.,} \end{cases} \tag{84}$$

we would obtain a restriction on the domain wall height M_0 from $\rho = 1/2$. This can be avoided by simply rescaling D_{eff} by a factor $\varrho = 2\rho$, so that—up to discretization effects—the low-lying eigenvalues of the kernel remain invariant under the effective operator projection in the free-field case. This is also illustrated in Fig. 8, which we elaborate on in Sec. VI A. Consequently, we will employ this rescaling in all our numerical investigations.

C. Approximate sign functions

The effective Dirac operators in the various formulations are given in terms of different sign function approximations. Explicitly, these approximations of sign (z) read

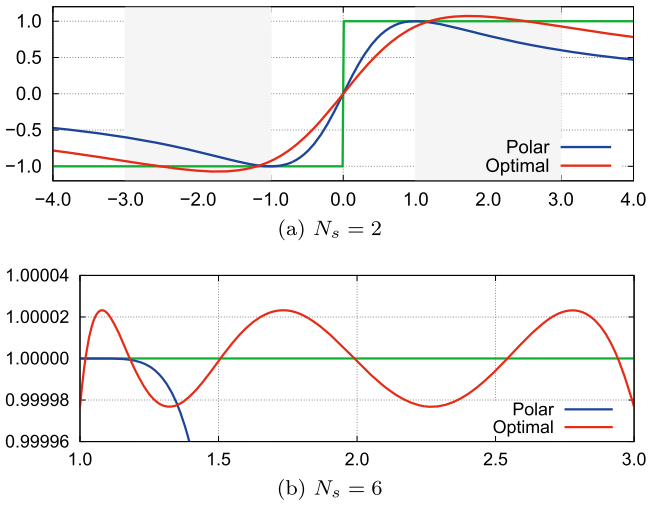

FIG. 1. Approximation of sign (z) by $r(z)$. The optimal construction was done for $\lambda_{\mathrm{min}} = 1$, $\lambda_{\mathrm{max}} = 3$.

$$r(z) = \frac{\Pi_+(z) - \Pi_-(z)}{\Pi_+(z) + \Pi_-(z)} \tag{85}$$

with

$$\Pi_\pm(z) = \begin{cases} (1 \pm z)^{N_s} & \text{for standard/Boriçi's constr.,} \\ \prod_s (1 \pm \omega_s z) & \text{for optimal constr.,} \end{cases} \tag{86}$$

so that $r(z) \to \mathrm{sign}(z)$ for $N_s \to \infty$. We illustrate these approximations in Fig. 1, comparing the polar decomposition approximation in Boriçi's construction with the optimal rational function approximation in Chiu's construction. The coefficients $\{\omega_s\}$ are directly linked to Zolotarev's coefficients, cf. Refs. [53,56,57]. Note that the sign function approximation for the standard construction agrees with the one in Boriçi's construction, but is applied to H_{m} rather than H_{w}.

Staggered formulations.—As previously suggested in Ref. [32], all central equations in this section generalize to the case of staggered Wilson fermions after the replacements given in Eq. (65). In particular, staggered domain wall fermions can be seen as a truncation of Neuberger's overlap construction with staggered Wilson kernel [32].

V. SETTING

In the following, we elaborate on the setting of our numerical simulations. In particular, we discuss our approach of comparing the chiral properties of the different formulations.

A. Choice of M_0

In the free-field case, suitable choices for the domain wall height M_0 are in the range $0 < M_0 < 2$ for a one flavor theory. In a gauge field background, in general this interval contracts. Intuitively, the parameter M_0 has to be chosen in such a way, that the origin is shifted sufficiently close to the center of the leftmost "belly" of the eigenvalue spectrum. While there is no unique optimal choice even in the free-field case [74], one can use the canonical choice $M_0 = 1$, which shifts the origin exactly to the center. To be more precise, the mobility edge [75–78] is the decisive quantity determining valid choices of M_0.

In the Schwinger model, the interval of valid choices for M_0 remains close to the free-field case for reasonable values of the inverse coupling β. In particular, $M_0 = 1$ remains a sensible and simple choice, which we are consequently using for all numerical work presented. This is in contrast to QCD in $3+1$ dimensions, where one commonly sets $M_0 = 1.8$ (see e.g. Ref. [79]).

B. Effective mass

Two common approaches found in the literature to quantify the induced effects of chiral symmetry breaking in domain wall fermions are the determination of the residual mass m_{res} [21,27,79,80] and the effective mass m_{eff} [81–83]. The former employs the explicit fermion mass dependence in the chiral Ward-Takahashi identities, while the latter is given by the lowest eigenvalue of the Hermitian operator in a topologically nontrivial background field. Although the definitions are not equivalent, their numerical values usually agree within a factor of $\mathcal{O}(1)$ and hence both are suitable to quantify the degree of chiral symmetry breaking.

In this work, we use the effective mass m_{eff} due to its conceptual simplicity. We hence define the effective mass for a given Dirac operator D with periodic boundary conditions in a topologically nontrivial background field as the lowest eigenvalue of the corresponding Hermitian version H of the Dirac operator. Noting that $H^2 = D^\dagger D$, we define

$$m_{\mathrm{eff}} = \min_{\lambda \in \mathrm{spec}H} |\lambda| = \min_{\Lambda \in \mathrm{spec}D^\dagger D} \sqrt{\Lambda}\,. \tag{87}$$

If D is a normal operator, then $m_{\mathrm{eff}} = \min_{\lambda \in \mathrm{spec}D} |\lambda|$. In the general case, however, there is no direct link between the eigenvalues of H and D.

On a topological nontrivial background configuration with topological charge $Q \neq 0$, the Atiyah-Singer index theorem [84–87] ensures the existence of zero modes of H in the continuum. The corresponding lattice version of this theorem [8–10] ensures that the overlap operator in Eq. (80) has exact zero modes as well. For domain wall fermions and their respective effective operators these zero modes are recovered in the $N_s \to \infty$ limit. For finite N_s, however, these zero modes become approximate and their deviation from zero can serve as a measure for the degree of chiral symmetry breaking.

If $n_\mp$ refers to the number of left-handed and right-handed zero modes, then the Atiyah-Singer index theorem states that

$$n_- - n_+ = (-1)^{d/2} Q, \tag{88}$$

see Ref. [31]. A precise definition of Q will be given in Eq. (92). We note here that in $1+1$ dimensions the Vanishing Theorem holds [88–90]. That is, if $Q \neq 0$, then either n_- or n_+ vanishes.

C. Normality and Ginsparg-Wilson relation

In the continuum, the Dirac operator is normal. The same holds for the naïve and staggered discretizations as well as for the overlap operator. The (staggered) Wilson kernel and the (staggered) domain wall fermion operators, on the other hand, are not normal.

As it has been shown that normality is necessary for chiral properties [91] (see also Refs. [92,93]), the degree of violation of normality is an interesting quantity in the context of chiral symmetry.

Let us recall that a normal operator D satisfies $[D, D^\dagger] = 0$ by definition. We then consider the quantity

$$\Delta_{\mathsf{N}} = \|[D, D^\dagger]\|_\infty, \tag{89}$$

where $\|\cdot\|_\infty$ is the by the L_∞-norm induced matrix norm. We know that Δ_{N} has to vanish for the effective operators introduced in Sec. IV in the limit $N_s \to \infty$.

Similarly, we consider violations of the Ginsparg-Wilson relation given in Eq. (82). The quantity

$$\Delta_{\mathsf{GW}} = \|\{\gamma_3, D\} - \rho^{-1} D \gamma_3 D\|_\infty, \tag{90}$$

has to vanish in the limit $N_s \to \infty$ as well. As before, we replace γ_3 by ϵ in the case of a staggered Wilson kernel. As previously already considered in Refs. [74,94], Δ_{N} and Δ_{GW} will give us a measure for the degree of chiral symmetry violation of the Dirac operators under consideration.

D. Topological charge

We determine the topological charge of the gauge configurations via both the standard overlap definition,

$$Q = \frac{1}{2}\mathrm{Tr}\left(H_{\mathsf{w}}/\sqrt{H_{\mathsf{w}}^2}\right), \tag{91}$$

and its staggered counterpart,

$$Q = \frac{1}{2}\mathrm{Tr}\left(H_{\mathsf{sw}}/\sqrt{H_{\mathsf{sw}}^2}\right), \tag{92}$$

with $H_{\mathrm{sw}} = \epsilon D_{\mathrm{sw}}(-M_0)$ as derived in Ref. [31]. On the small sample of gauge configurations considered in this paper, they were found to be in exact agreement. Although a more careful investigation of the continuum limit would be needed, this observation is consistent with analytical results [95] and other numerical studies [41,96].

VI. NUMERICAL RESULTS

We are now moving to the numerical part of this work. We calculate the complete eigenvalue spectra of all Dirac operators introduced in the previous sections, both with a Wilson and staggered Wilson kernel, for the $(1+1)$-dimensional Schwinger model. We consider the free-field case, thermalized gauge configurations and the smooth topological configurations constructed in Ref. [97].

In the following, we set the lattice spacing to $a = a_{d+1} = 1$ and Wilson parameter to $r = 1$. The extent in the extra dimension will be varied in the range $2 \leq N_s \leq 8$. We use periodic boundary conditions in both space and time direction, so that the determination of the effective mass m_{eff} as defined in Sec. V B applies.

Extremal eigenvalues are determined with ARPACK [98], while complete spectra are computed with LAPACK [99]. Calculations are carried out in double precision. In all figures, the abbreviation "std" refers to the standard construction, "Bor" to Boriçi's construction and "opt" to Chiu's optimal construction. With respect to the overlap constructions, "DW" refers to the overlap operator with kernel H_{m}, "Neub" to Neuberger's overlap with kernel H_{w} and "Adams" to Adams' staggered overlap with kernel H_{sw}.

A. Free-field case

We begin with the free-field case. Here we can employ a momentum space representation of the kernel. In particular, the Wilson kernel can be represented as a 2×2 linear map

$$D_{\mathrm{w}} = (m_{\mathrm{f}} + 2r)\mathbb{1} + \mathrm{i}\sum_{\mu}\gamma_\mu \sin p_\mu - r\sum_{\nu}\cos p_\nu \mathbb{1}, \qquad (93)$$

where $p_\mu = 2\pi n_\mu / N_\mu$ with $n_\mu = 0, 1, \ldots, N_\mu - 1$ and N_μ is the number of slices in μ-direction. The staggered Wilson kernel takes the form of the 4×4 linear map

$$D_{\mathrm{sw}} = m_{\mathrm{f}}(\mathbb{1} \otimes \mathbb{1}) + \mathrm{i}\sum_{\mu}\sin p_\mu(\gamma_\mu \otimes \mathbb{1}) + r\mathbb{1} \otimes \left(\mathbb{1} + \xi_3 \prod_{\nu}\cos p_\nu\right) \qquad (94)$$

with $n_\mu = 0, 1, \ldots, N_\mu/2 - 1$ (see also Refs. [41,95]).

In the three-dimensional operators, we keep the extra dimension in the position space formulation, as in general it is lacking periodicity. Besides reducing the dimensionality of the eigenvalue problem by choosing a momentum space representation for the kernel, this also avoids some numerical instabilities of the free-field case encountered in a purely position space based formulation.

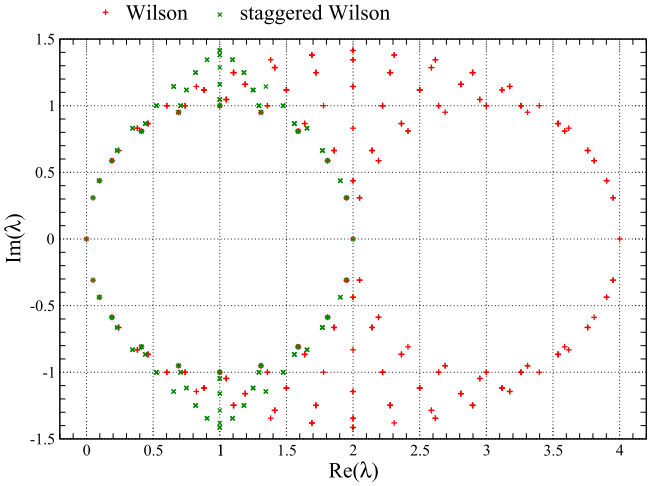

FIG. 2. Free-field spectrum of kernel operators.

In the following, all numerical results are for the case of a $N_s \times N_t = 20 \times 20$ lattice.

Kernel operators.—In Fig. 2, we can find the well known free spectra of the kernel operators. In $1+1$ dimensions, the Wilson Dirac operator has only two doubler branches in the eigenvalue spectrum due to the reduced number of fermion species in this low-dimensional setting. Like in $3+1$ dimensions, the staggered Wilson Dirac operator has a single doubler branch due to the splitting of positive and negative flavor-chirality species.

One can see that the free-field spectrum of the staggered Wilson kernel is closer to the Ginsparg-Wilson circle compared to the Wilson kernel. One can then hope for a better performance of chiral formulations with this kernel, at least on sufficiently smooth configurations.

The bulk and effective operators, which we are going to discuss in the following, use either a Wilson or a staggered Wilson kernel. Comparing both cases, we note that the spectra of these operators differ mostly due to the different ultraviolet parts of the respective kernel spectra. Although the low-lying parts of the kernel spectrum in the physical branch are alike, the ultraviolet modes will alter the resulting spectrum of the bulk and effective operators differently and have an impact on the efficiency and chiral properties.

Bulk operators.—In Figs. 3 and 4, we show the spectrum of the $(2+1)$-dimensional bulk operator in the standard, Boriçi's and the optimal construction. In Fig. 5, we show periodic $(m = -1)$ and antiperiodic $(m = 1)$ boundary conditions in the extra dimension to compare with the Dirichlet $(m = 0)$ case.

We can observe that the bulk spectra for Boriçi's and the optimal construction have lost their resemblance to a Wilson operator in three dimensions. Specifically, while for the standard construction we find (two) three doubler

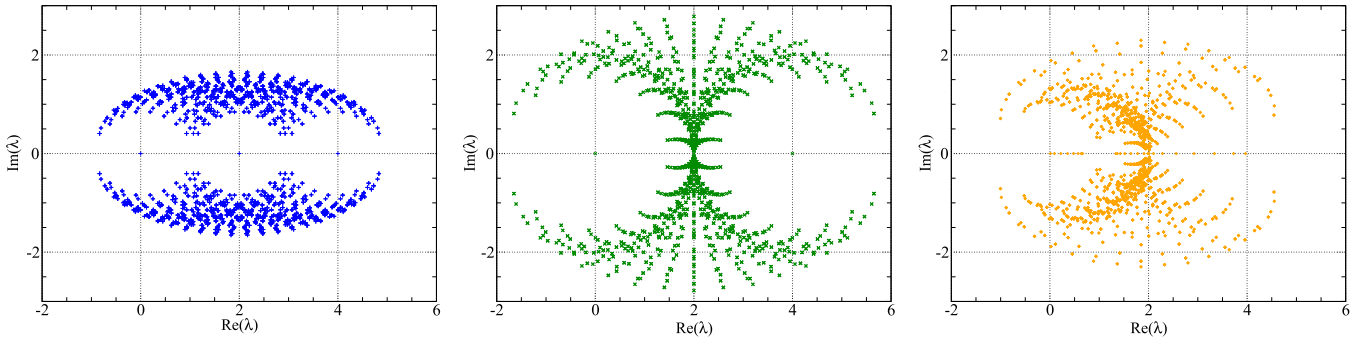

(a) Standard construction (b) Boriçi's construction (c) Optimal construction

FIG. 3. Free-field spectrum of D_{dw} with Wilson kernel for $m = 0$ at $N_s = 8$.

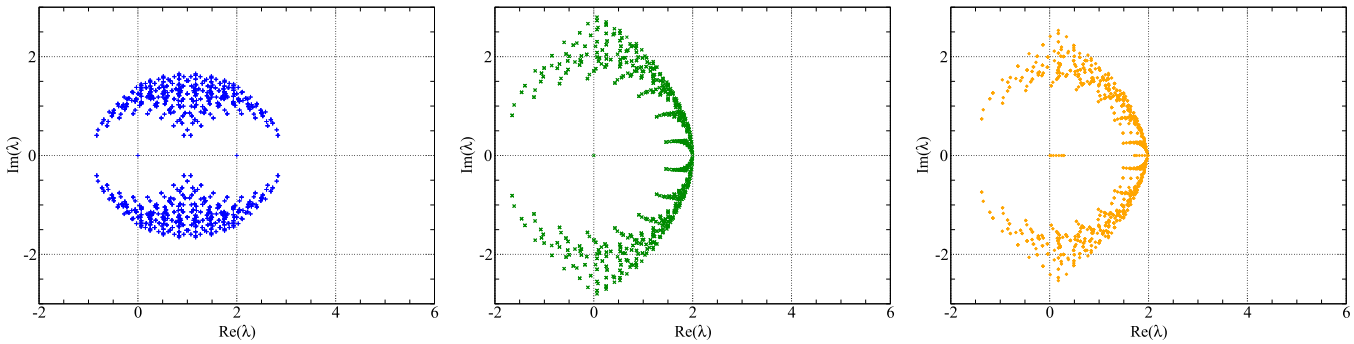

(a) Standard construction (b) Boriçi's construction (c) Optimal construction

FIG. 4. Free-field spectrum of D_{sdw} with staggered Wilson kernel for $m = 0$ at $N_s = 8$.

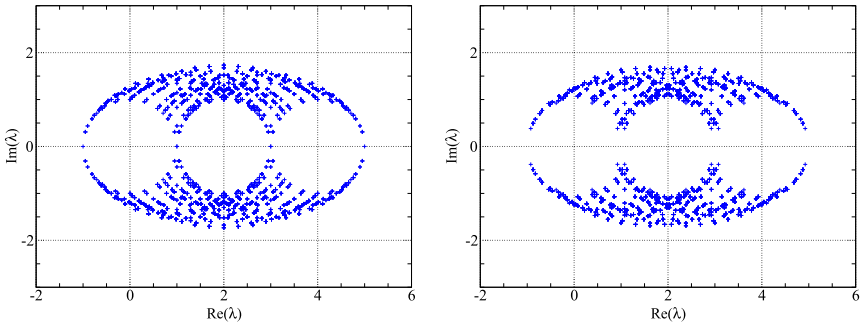

(a) Periodic case ($m = -1$) (b) Antiperiodic case ($m = 1$)

FIG. 5. Free-field spectrum of D_{dw} with Wilson kernel in the standard construction with different boundary conditions at $N_s = 8$ (cf. Fig. 3).

branches in the spectrum with the (staggered) Wilson kernel, in Boriçi's construction one less branch is visible. In the standard and Boriçi's construction, we find $2N_s$ exact zero modes in the Dirichlet case [20,81], which disappear for $m \neq 0$. In the optimal construction, we notice how the corresponding eigenvalues get spread out along the real axis and we are left with only two approximate zero modes.

Effective operators.—We now move on to the effective operators ϱD_{eff} as defined in Eq. (75). In Figs. 6 and 7, we show the respective eigenvalue spectra with a Wilson and staggered Wilson kernel.

As we can see, the spectra approach the Ginsparg-Wilson circle rapidly for increasing values of N_s. This fast convergence is of course expected on smooth configurations like the free field. Already for $N_s = 8$ the spectrum is close to the spectrum of the corresponding overlap operator in the $N_s \to \infty$ limit. In particular, we note the rapid convergence of Boriçi's and Chiu's construction with a staggered Wilson kernel.

The effective Dirac operator in the optimal construction shows a significantly improved convergence. Let us recall that for a given interval $I = [\lambda_{\mathrm{min}}, \lambda_{\mathrm{max}}]$ the optimal rational

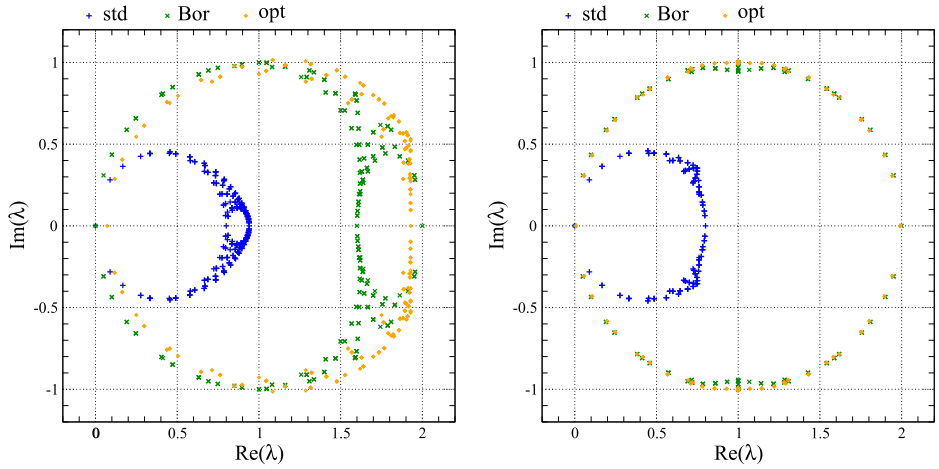

(a) Wilson kernel (b) Staggered Wilson kernel

FIG. 6. Spectrum of ϱD_{eff} at $N_s = 2$ for the standard (std), Boriçi (Bor) and optimal (opt) construction.

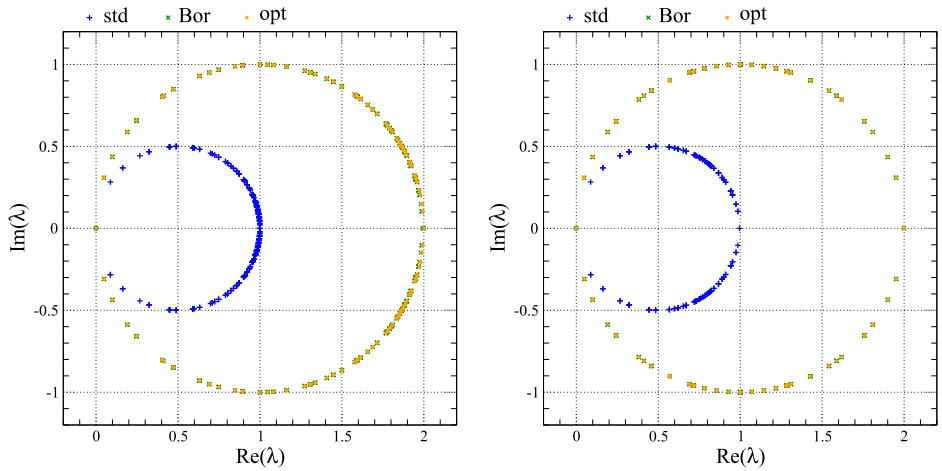

(a) Wilson kernel (b) Staggered Wilson kernel

FIG. 7. Spectrum of ϱD_{eff} at $N_s = 8$ for the standard (std), Boriçi (Bor) and optimal (opt) construction.

function approximation $r_{\mathrm{opt}}(z)$ of the sign function minimizes the maximal deviation

$$\delta_{\mathrm{max}} = \max_{z \in -I \cup I} |\mathrm{sign}(z) - r_{\mathrm{opt}}(z)| = 1 \mp r_{\mathrm{opt}}(\pm\lambda_{\mathrm{min}}) \tag{95}$$

on the domain $-I \cup I$. As expected, we observe that all eigenvalues lie within a tube with diameter $2\delta_{\mathrm{max}}$ around the Ginsparg-Wilson circle. That is, for all eigenvalues λ we find $||\lambda| - 1| \leq \delta_{\mathrm{max}}$. Noting that the sign function has a point of maximal deviation at both λ_{min}, we observe the absence of an exact zero mode in contrast to the standard and Boriçi's construction. However, due to the rapid convergence of the rational function approximation, the approximate zero mode is of small magnitude for already moderate values of N_s.

Overlap operators.—In the $N_s \to \infty$ limit, the effective operators can be formulated as overlap operators defined in Eq. (80) with the kernel H given in Eq. (74). In Fig. 8, we can find the spectra of ϱD_{ov} together with the stereographic projection π of the eigenvalues onto the imaginary axis via

$$\pi(\lambda) = \frac{\lambda}{1 - \frac{1}{\varrho}\lambda}. \tag{96}$$

We also point out the high degree of symmetry of the spectrum in the case of Adams' overlap. As noted before, the effective Dirac operators in Boriçi's and the optimal construction converge towards Neuberger's and Adams' overlap operator for $N_s \to \infty$, while in the standard construction, we find a modified overlap kernel.

B. U(1) gauge field case

While the free field is an interesting case, our main interest is the performance of the Dirac operators in nontrivial background fields. Dealing with the Schwinger

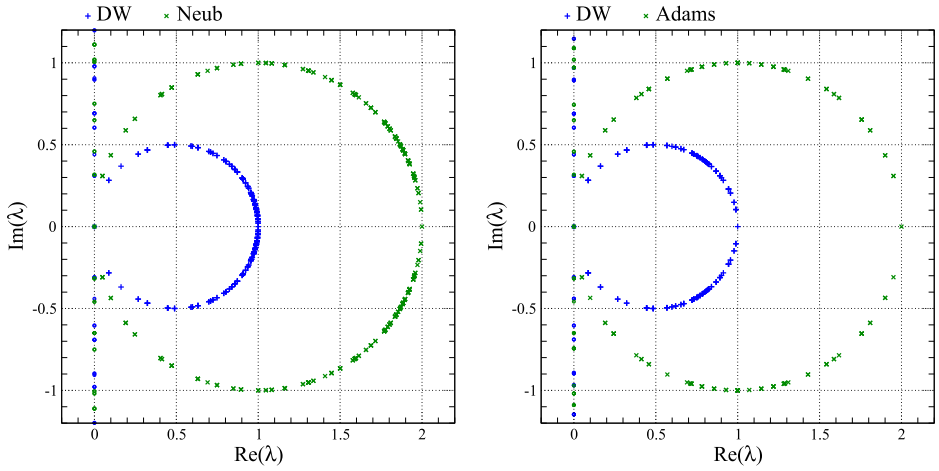

(a) Wilson kernel (b) Staggered Wilson kernel

FIG. 8. Spectrum of ϱD_{ov} with stereographic projection for domain wall (DW) and standard (Neub/Adams) kernels.

model, for the rest of the work we consider U(1) gauge fields. We use quenched thermalized gauge fields following the setup of Refs. [100,101]. Note that while these gauge fields originate from a quenched ensemble, there is no problem in the Schwinger model to reweight them to an arbitrary mass unquenched ensemble [100–103].

In this section, we start our investigation by focusing on a few individual 20^2 configurations at an inverse coupling of $\beta = 5$ to illustrate the qualitative features of the spectra.

Kernel operators.—In Fig. 9, we can see the kernel spectra in a gauge background with $Q = 1$. As expected in the Schwinger model, the branches stay much sharper and well separated compared to the $(3 + 1)$-dimensional QCD case [40–43].

Bulk operators.—In Figs. 10 and 11, we show the spectra of the bulk operators on the same gauge configuration as used in Fig. 9. Due to the use of a gauge configuration with $Q \neq 0$, the effective operator is guaranteed to have $|Q|$ exact zero modes in the limit $N_s \to \infty$. In this setting, we find $N_s \cdot |Q|$ eigenvalues in the vicinity of the origin in the bulk spectrum, which are linked to these zero modes. We can also see how the optimal construction distorts the spectrum, effectively improving chiral properties and resulting in a reduced m_{eff}.

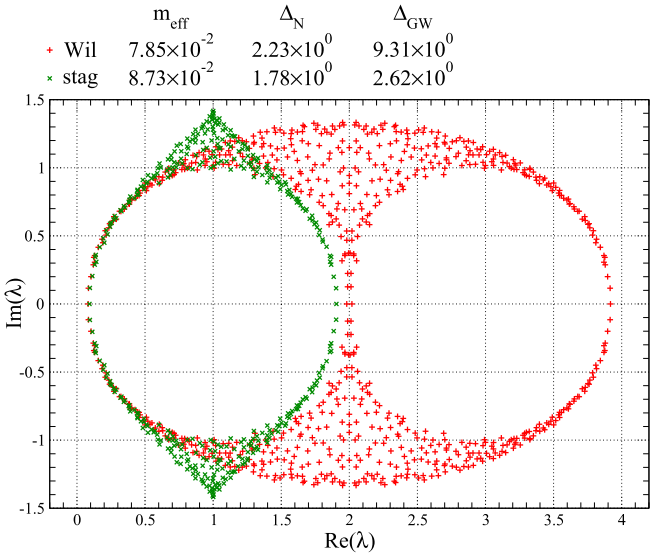

FIG. 9. Spectrum of kernel operators.

Effective operators.—In Figs. 12 and 13, we plot the spectra of the effective operators on the same gauge field background as used in Fig. 9. We note that for $N_s \geq 4$ Boriçi's construction outperforms the standard construction with respect to all measures m_{eff}, Δ_{N} and Δ_{GW}.

The optimal construction decreases most of these numbers even further. In Fig. 13(b), we see that m_{eff} is already comparable to the round-off error and, hence, we only quote an upper bound. Note that as in a U(1) background field the kernel operator is in general not normal, the inequality $||\lambda| - 1| \leq \delta_{\mathrm{max}}$ does not have to be saturated. Moreover it is evident that a smaller maximum deviation δ_{max} from the sign function on a given interval does not necessarily translate to a smaller Δ_{GW}, although there is a strong correlation. For larger N_s this problem is cured by the fast convergence of optimal domain wall fermions.

Let us remark that optimal domain wall fermions are optimal in a very particular sense, namely the minimization of δ_{max} as defined in Eq. (95). As Ref. [66] suggests, they are not optimal with respect to e.g. the number of iterations needed for solving a linear system. In principle, one could also formulate domain wall fermions optimized with respect to other measures, such as the minimization of Δ_{GW} (which, however, might require more knowledge about the spectrum).

Comparing domain wall fermions with a Wilson and staggered Wilson kernel, we can see that in the case of the standard construction m_{eff}, Δ_{N} and Δ_{GW} are usually of the same magnitude. However, for Boriçi's and the optimal

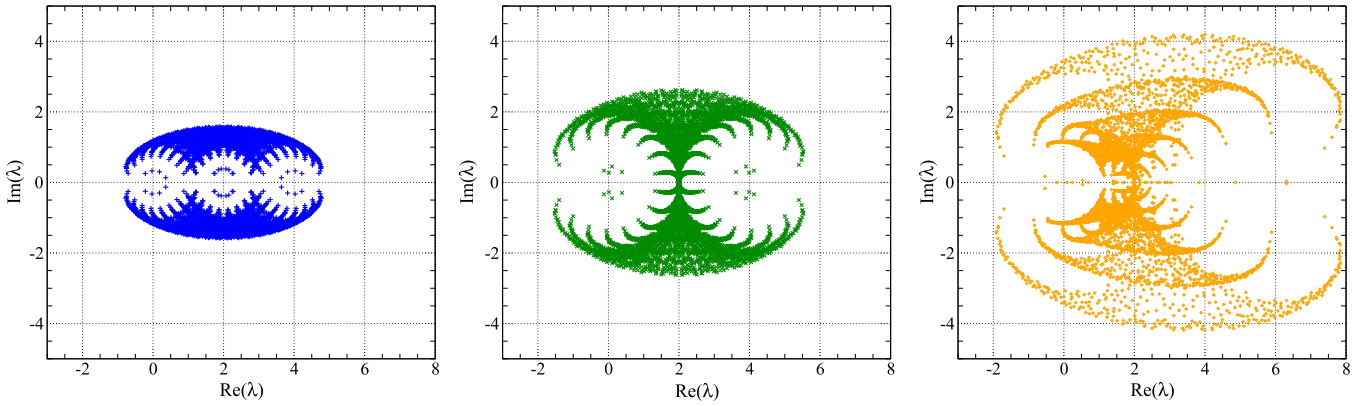

(a) Standard construction (b) Boriçi's construction (c) Optimal construction

FIG. 10. Spectrum of D_{dw} with Wilson kernel for $m = 0$ at $N_s = 8$.

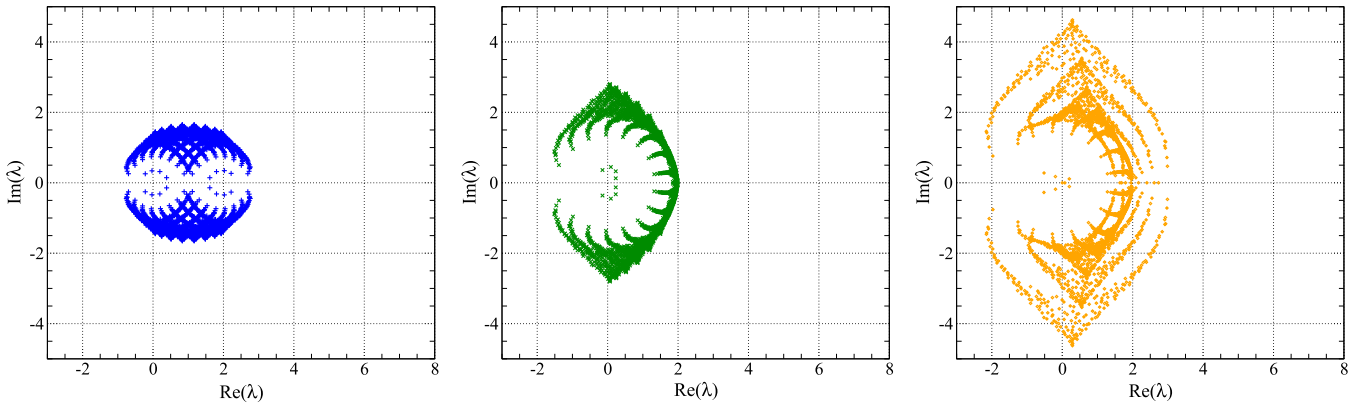

(a) Standard construction (b) Boriçi's construction (c) Optimal construction

FIG. 11. Spectrum of D_{sdw} with staggered Wilson kernel for $m = 0$ at $N_s = 8$.

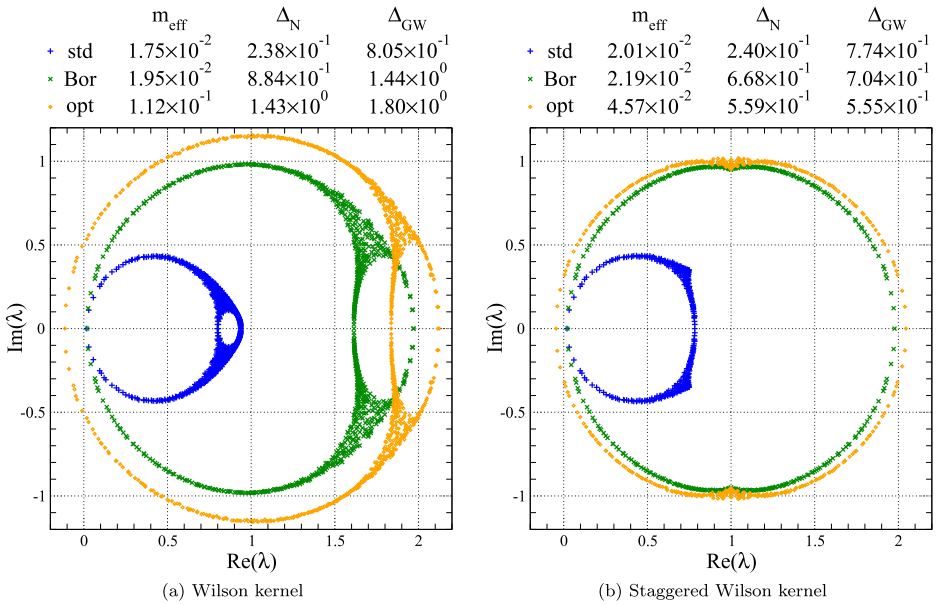

(a) Wilson kernel (b) Staggered Wilson kernel

FIG. 12. Spectrum of ϱD_{eff} at $N_s = 2$ for the standard (std), Boriçi (Bor) and optimal (opt) construction.

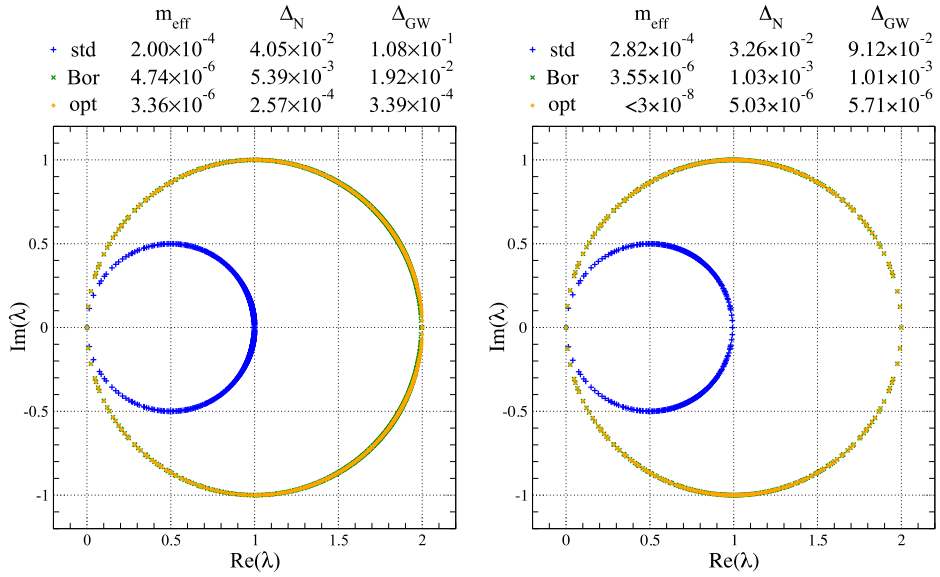

(a) Wilson kernel (b) Staggered Wilson kernel

FIG. 13. Spectrum of ϱD_{eff} at $N_s = 8$ for the standard (std), Boriçi (Bor) and optimal (opt) construction.

construction a staggered Wilson kernel seems to outperform the usual Wilson kernel in terms of chiral symmetry violations in the U(1) background fields under consideration.

For the rather artificial case $N_s = 2$ we can make some interesting observations. While for a staggered Wilson kernel the relative performances of all formulations under consideration is comparable, for a Wilson kernel the standard formulation performs better than Boriçi's and markedly better than optimal.

Overlap operators.—In Fig. 14, we show the corresponding overlap operators together with the stereographic projection of the spectrum. All of the quantities m_{eff}, Δ_{N} and Δ_{GW} vanish in exact arithmetic and are, therefore, omitted in the figure labels.

C. Smearing

In realistic simulations, smearing is a commonly employed technique. As suggested in Ref. [42], it is expected to be especially beneficial when employing a staggered Wilson kernel (in $3+1$ dimensions, this is more pronounced). Hence, we consider three-step APE smeared [104,105] gauge field backgrounds with a smearing parameter $\alpha = 0.5$, which is the maximal value within the perturbatively reasonable range in two dimensions [106].

As a first test on the impact on the performance of staggered domain wall fermions, we can find a direct comparison at $N_s = 4$ in Figs. 15 and 16 between an unsmeared and a smeared version of a configuration both for a Wilson and a staggered Wilson kernel. As we can see,

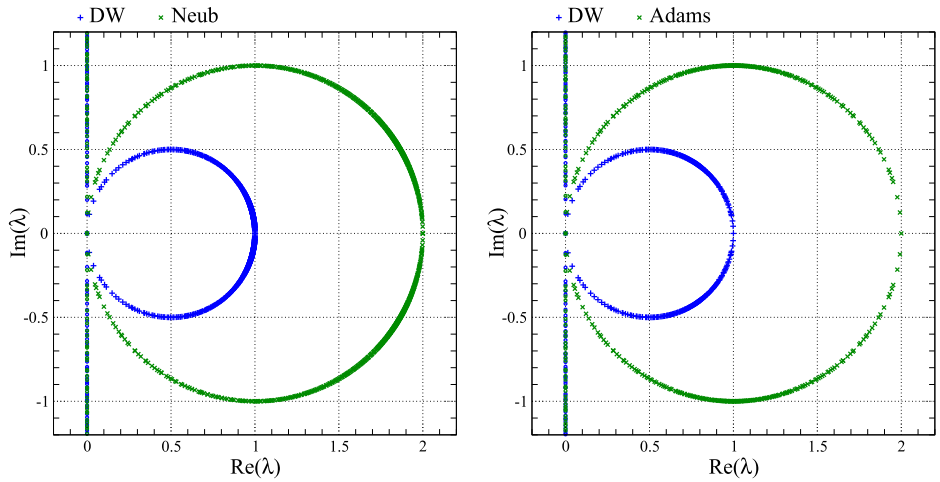

(a) Wilson kernel (b) Staggered Wilson kernel

FIG. 14. Spectrum of ϱD_{ov} with stereographic projection for domain wall (DW) and standard (Neub/Adams) kernels.

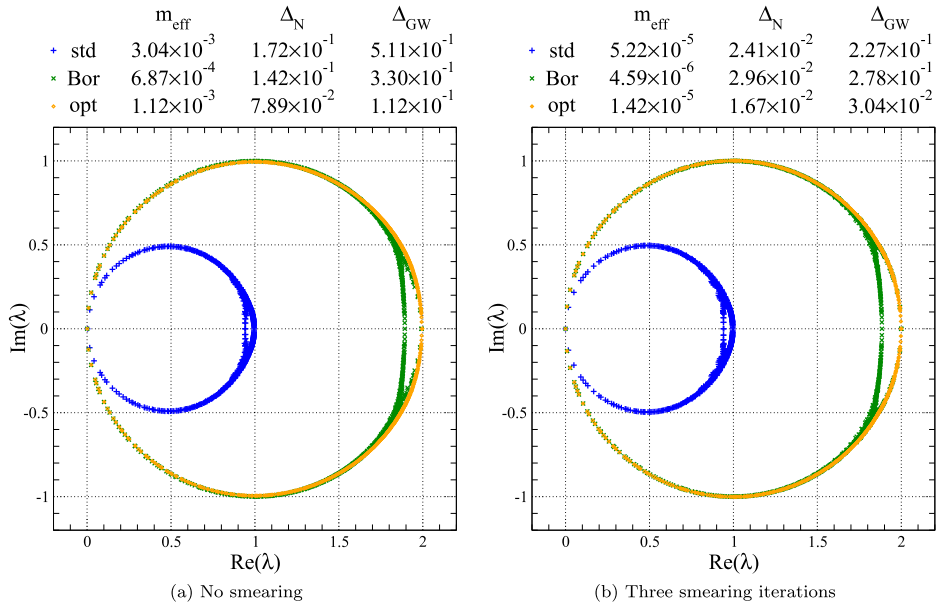

(a) No smearing (b) Three smearing iterations

FIG. 15. Spectrum of ϱD_{eff} with Wilson kernel and smearing parameter $\alpha = 0.5$ at $N_s = 4$ for the standard (std), Boriçi (Bor) and optimal (opt) construction.

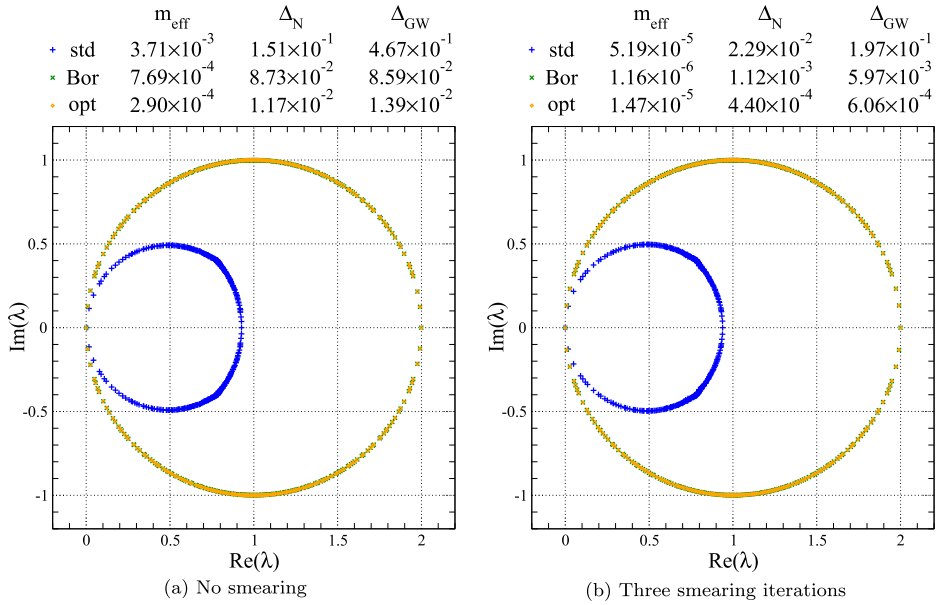

(a) No smearing (b) Three smearing iterations

FIG. 16. Spectrum of ϱD_{eff} with staggered Wilson kernel and smearing parameter $\alpha = 0.5$ at $N_s = 4$ for the standard (std), Boriçi (Bor) and optimal (opt) construction.

with three smearing steps, m_{eff}, Δ_{N} and Δ_{GW} get reduced significantly—in some cases up to 2 orders of magnitude—with the exception of m_{eff} for standard domain wall fermions with Wilson kernel.

D. Topology

As discussed earlier, for topological charges $Q \neq 0$, the Atiyah–Singer index theorem guarantees the existence of zero modes of the continuum Dirac operator. On the lattice one can show the same for the overlap operators defined in Eq. (80). As a consequence we observe approximate zero modes in the eigenvalue spectra of the effective operators ϱD_{eff} as illustrated in Fig. 17. As the Vanishing Theorem holds in $1+1$ dimensions, we find these modes with a multiplicity of $|Q|$.

In addition, we can study topological aspects by employing the method in Ref. [97] to construct gauge configurations with given topological charge Q. These smooth configurations are fixed points with respect to the APE smearing prescription. We construct these configurations

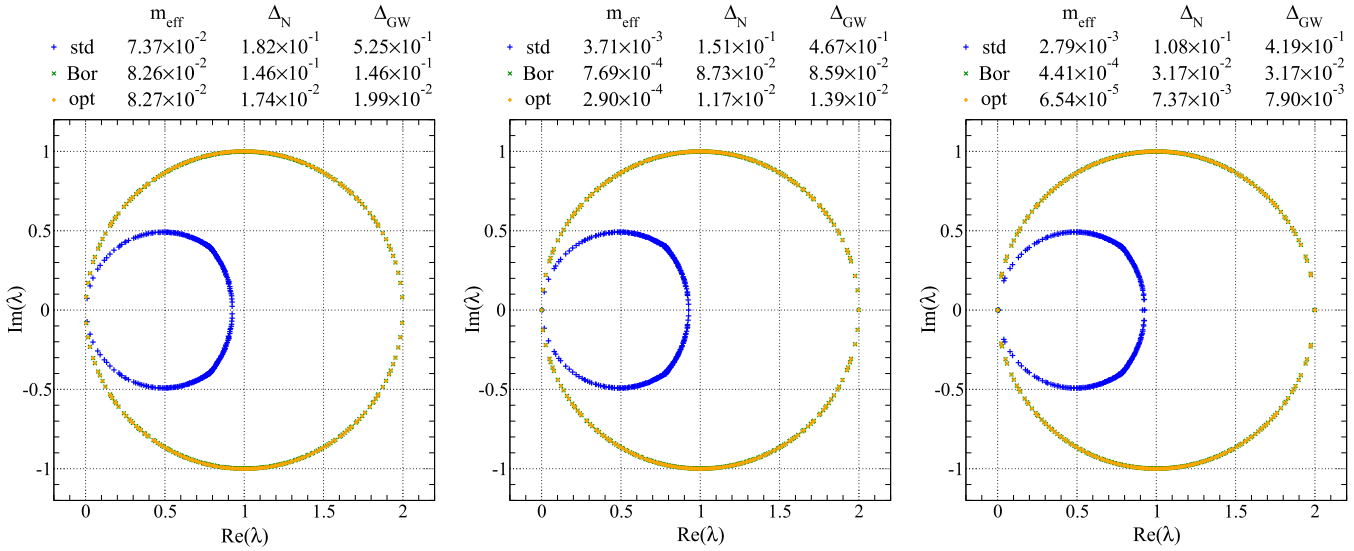

(a) Configuration with $Q = 0$ (b) Configuration with $Q = 1$ (c) Configuration with $Q = 3$

FIG. 17. Spectrum of ϱD_{eff} with staggered Wilson kernel for various topological charges Q at $N_s = 4$ for the standard (std), Boriçi (Bor) and optimal (opt) construction.

for a wide range of topological charges Q and evaluate the measures m_{eff}, Δ_{N} and Δ_{GW} for the effective operators. In this setting, these measures are equal within numerical rounding errors for topological charge $\pm Q$ and, thus, only depend on $|Q|$.

We find that m_{eff}, Δ_{N} and Δ_{GW} are very small in magnitude on these specific configurations compared to thermalized configurations. Moreover, they increase with larger values of $|Q|$. In Fig. 18, we can see two examples of bulk spectra on a 20^2 lattice, which reveal a very clear structure on these smooth background fields.

E. Spectral flow

Another tool to investigate topological aspects on the lattice, such as the index theorem, is the spectral flow [4,107].

In the case of a Wilson kernel, one considers the eigenvalues $\{\lambda(m_{\text{f}})\}$ of the Hermitian operator $H_{\text{w}}(m_{\text{f}})$ as a function of m_{f}. One can show that there is a one-to-one correspondence between the eigenvalue crossings of $H_{\text{w}}(m_{\text{f}})$ and the real eigenvalues of $D_{\text{w}}(m_{\text{f}})$. Furthermore the low-lying real eigenvalues of $D_{\text{w}}(m_{\text{f}})$ correspond to the would-be zero modes [97] and one can show that for these modes the slope of the eigenvalue crossings in the vicinity of $m_{\text{f}} = 0$ equals minus the chirality. By identifying the eigenvalues crossings occurring at small values of m_{f} as well as their slopes, one can then infer the topological charge Q of the gauge field.

While originally the spectral flow was used for a Wilson kernel, eventually the applicability to the staggered case could be shown as well [31,40,41,96,108]. Spectral flows of both the Wilson and staggered Wilson kernel have been investigated in the literature before. Here we want to illustrate the effectiveness of smearing.

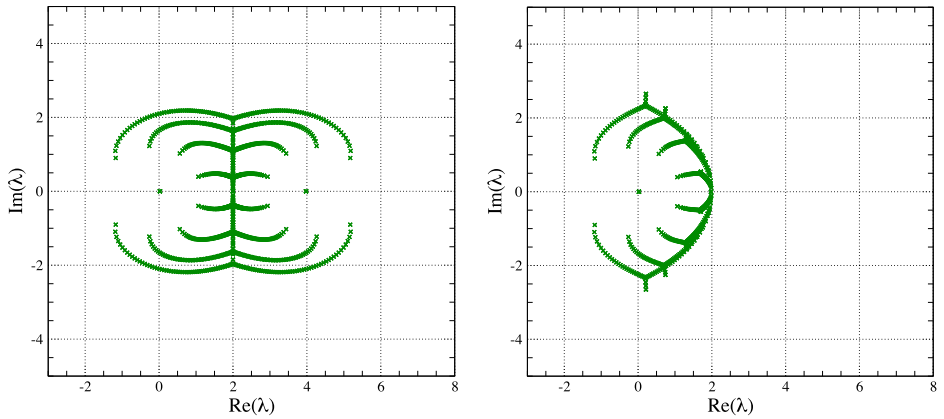

(a) Wilson kernel (b) Staggered Wilson kernel

FIG. 18. Spectrum of D_{dw} in Boriçi's construction at $N_s = 4$ for a topological configuration with $Q = 3$.

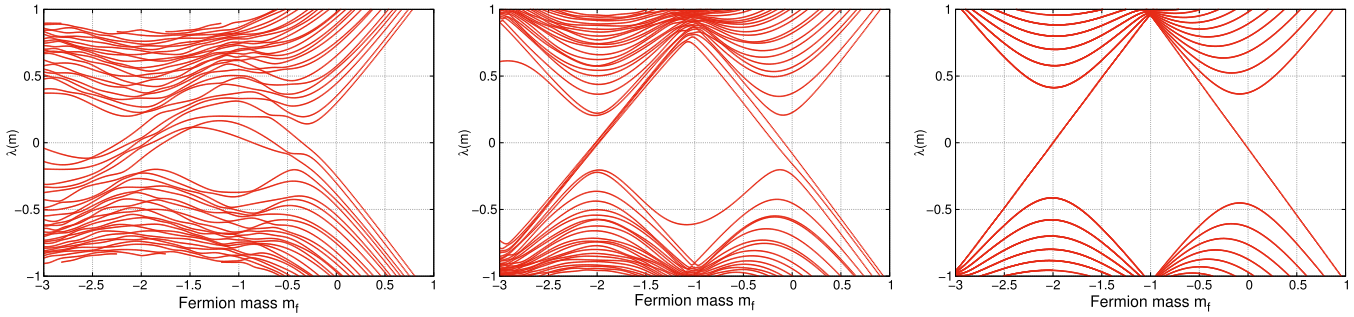

(a) Unsmeared configuration (b) Smeared configuration (c) Topological configuration

FIG. 19. Spectrum of the Wilson kernel for gauge fields with $Q = 2$.

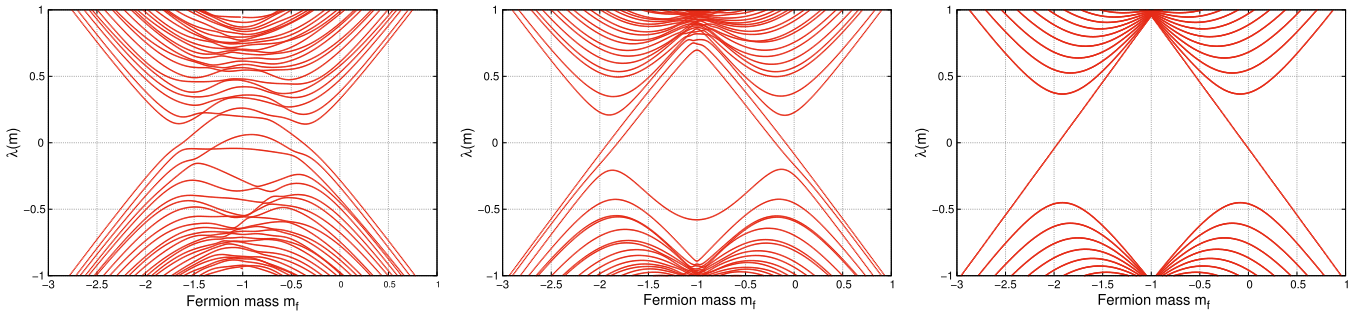

(a) Unsmeared configuration (b) Smeared configuration (c) Topological configuration

FIG. 20. Spectrum of the staggered Wilson kernel for gauge fields with $Q = 2$.

In Figs. 19 and 20, we show the eigenvalue flow $\lambda(m_f)$ of $H_w(m_f)$ and $H_{sw}(m_f)$ for the lowest 50 eigenvalues. We consider a 12^2 gauge configuration at $\beta = 1.8$ with topological charge $Q = 2$. We calculate the eigenvalue flow on the unsmeared and three-step APE smeared configuration with smearing parameter $\alpha = 0.5$. For comparison, we also show the corresponding topological gauge configuration described in Sec. VI D. As one can see, the use of smearing allows the unambiguous determination of the topological charge Q, which on the rough configuration without

TABLE I. Median values for the chiral symmetry violations on unsmeared 32^2 configurations at $\beta = 12.8$.

Kernel	Construction	N_s	m_{eff}	Δ_N	Δ_{GW}
Wilson	Standard	2	5.47×10^{-3}	1.53×10^{-1}	6.72×10^{-1}
		4	5.90×10^{-4}	6.87×10^{-2}	3.10×10^{-1}
		6	1.00×10^{-4}	2.30×10^{-2}	1.02×10^{-1}
	Boriçi	2	5.73×10^{-3}	3.71×10^{-1}	1.16×10^{0}
		4	8.56×10^{-5}	6.64×10^{-2}	3.00×10^{-1}
		6	5.42×10^{-6}	1.57×10^{-2}	7.60×10^{-2}
	Optimal	2	8.30×10^{-3}	7.51×10^{-1}	1.16×10^{0}
		4	2.11×10^{-3}	3.59×10^{-2}	4.78×10^{-2}
		6	8.71×10^{-6}	1.21×10^{-3}	1.74×10^{-3}
Staggered Wilson	Standard	2	6.22×10^{-3}	1.48×10^{-1}	6.49×10^{-1}
		4	7.18×10^{-4}	5.88×10^{-2}	2.88×10^{-1}
		6	1.34×10^{-4}	2.01×10^{-2}	9.72×10^{-2}
	Boriçi	2	6.38×10^{-3}	2.02×10^{-1}	2.92×10^{-1}
		4	5.13×10^{-5}	5.45×10^{-3}	8.68×10^{-3}
		6	5.91×10^{-7}	1.53×10^{-4}	2.69×10^{-4}
	Optimal	2	1.72×10^{-2}	2.32×10^{-1}	2.66×10^{-1}
		4	3.35×10^{-5}	2.23×10^{-3}	2.63×10^{-3}
		6	5.02×10^{-8}	2.01×10^{-5}	2.36×10^{-5}

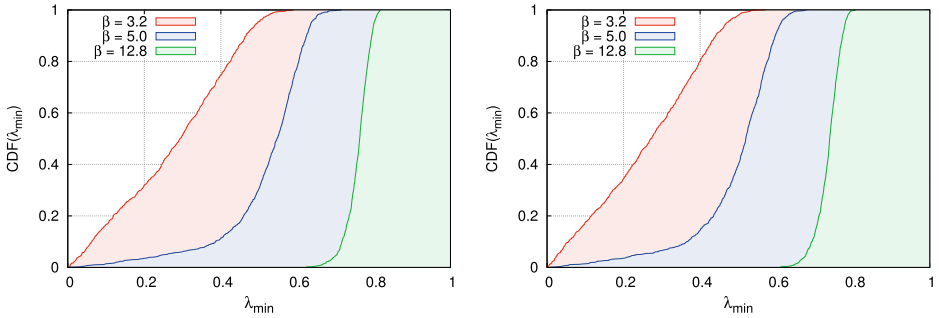

(a) Wilson kernel (b) Staggered Wilson kernel

FIG. 21. Cumulative distribution function CDF for λ_{min} of H_{w} and H_{sw}.

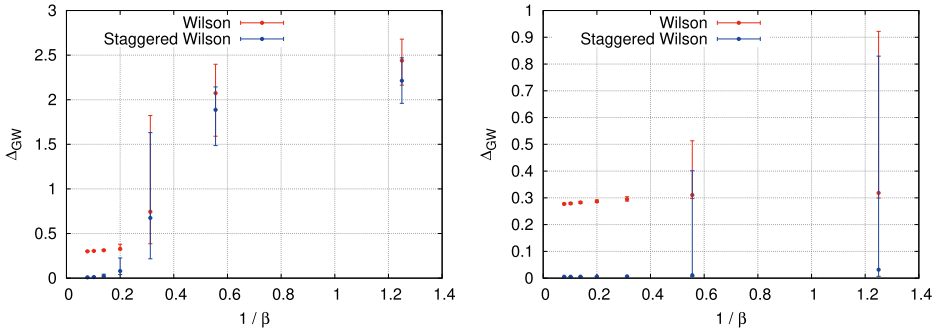

(a) Without smearing (b) With smearing

FIG. 22. Δ_{GW} of ϱD_{eff} in Boriçi's construction at $N_s = 4$ as a function of $1/\beta$.

smearing is otherwise difficult. Finally, the corresponding topological charge for $Q = 2$ is so smooth that the two eigenvalue crossings close to the origin lie on top of each other. This shows how beneficial the use of smearing is when studying topological aspect using spectral flows.

F. Approaching the continuum

In order to judge the performance of the different fermion formulations when approaching the continuum, we evaluated them on seven different ensembles with 1000 configurations each. We kept the physical volume constant and considered the following lattices: 8^2 at $\beta = 0.8$, 12^2 at $\beta = 1.8$, 16^2 at $\beta = 3.2$, 20^2 at $\beta = 5.0$, 24^2 at $\beta = 7.2$, 28^2 at $\beta = 9.8$ and 32^2 at $\beta = 12.8$. Together with the smeared version of each configuration, we consider $N = 14000$ configurations in total.

We do not attempt to carry out a strict continuum limit analysis, but we are interested in the relative performance of the different formulations when the lattices become finer. An indication for the performance are the chiral symmetry violations on our finest lattice at $\beta = 12.8$. We quote the median values in Table I. We restrict ourselves to $N_s \in \{2, 4, 6\}$ as for $N_s \geq 8$ some values have the same of order of magnitude as the rounding errors and, thus, we are unable to quote precise numbers. We observe that for large β the chiral symmetry violations for the standard construction are comparable in the case of a Wilson and a staggered Wilson kernel. For Boriçi's and the optimal construction, on the other hand, the violations are much lower for a staggered Wilson kernel, often by 1 to 2 orders of magnitude. Note that for simplicity we set the parameters λ_{min} and λ_{max} for optimal domain wall fermions on a configuration basis. This is intended to give an indication of the performance, while in realistic simulations one would fix suitable values on an ensemble basis after having projected out a number of low-lying eigenmodes. One then has to find a compromise between mapping small eigenvalues accurately and keeping the overall approximation error small.

In general, we also observe that the optimal construction shows a better performance than Boriçi's, while Boriçi's construction performs better than the standard construction. A interesting exception is m_{eff}, where the optimal construction with a Wilson kernel is not clearly outperforming the other constructions. This is not unexpected as the optimal sign-function approximation has a point of maximal deviation at λ_{min} and as a result low-lying eigenvalues are not mapped accurately on smooth configurations. However, for larger N_s this phenomenon disappears and the optimal construction shows a superior performance.

A related question is how the lowest eigenvalue $\lambda_{\mathrm{min}} = \min_{\lambda \in \mathrm{spec}H} |\lambda|$ of the kernel operators $H = H_{\mathrm{w}}$ and $H = H_{\mathrm{sw}}$ is distributed. Especially close to the origin

smooth approximations to the sign-function tend to be inaccurate, so the mappings of small eigenvalues suffer from large errors. In Fig. 21, we can find the numerically determined cumulative distribution functions (CDFs) for both kernel at three different β. As expected, for larger β the tail of small values thins out and near-zero λ_{min} become infrequent. The CDFs for the Wilson and staggered Wilson kernel look very much alike and the probability to encounter configurations where $\lambda_{\mathrm{min}} \approx 0$ is comparable.

Finally, an example of how chiral symmetry violations vary with β can be found in Fig. 22. We show here the violation of the Ginsparg-Wilson relation Δ_{GW} of ϱD_{eff} in Boriçi's construction at $N_s = 4$ as a function of $1/\beta$. We plot the median value together with the width of the distribution, characterized by the q-quantile and the $(1-q)$-quantile, where $q = [1 - \mathrm{erf}(1/\sqrt{2})]/2$ and erf denotes the error function. With this choice 68.3% of the values are within the error bars. One can clearly see how the effective operator with a staggered Wilson kernel shows superior chiral properties when β is sufficiently large. As expected, we observe that smearing improves chiral properties in particular on the coarsest lattices.

VII. CONCLUSIONS

In this work, we gave an explicit construction of staggered domain wall fermions and investigated some of their basic properties in the free-field case, on quenched thermalized gauge configurations in the Schwinger model and on smooth topological configurations. It appears that staggered domain wall fermions indeed work as advertised.

Moreover we could generalize existing modifications of domain wall fermions, such as Boriçi's and the optimal construction to the staggered case. This gives rise to previously not considered truncated staggered domain wall fermions and optimal staggered domain wall fermions. These modified staggered domain wall fermions in particular show significantly smaller chiral symmetry violations than the traditional Wilson based formulations, at least in our setting and with respect to the criteria used in this work. These properties make formulations with a staggered Wilson kernel potentially interesting when studying phenomena, where chiral symmetry is of importance.

It is not yet clear how our results in U(1) background gauge fields will translate to QCD in $3+1$ dimensions with a SU(3) gauge group, but they are encouraging and warrant further investigations.

ACKNOWLEDGMENTS

We thank Ting-Wai Chiu for helping us to validate our implementation of optimal domain wall fermions and Stephan Dürr for helpful comments on the manuscript. C. H. is supported by DFG grant SFB/TRR-55. C. Z. is supported by the Singapore International Graduate Award (SINGA) and Nanyang Technological University. Parts of the computations were done on the computer cluster of the University of Wuppertal.

APPENDIX: OPTIMAL WEIGHTS

In the following, we give some example values for the weight factors as defined in Sec. III C. To this end, let us consider the free-field case in $1+1$ dimensions with the particular choices $M_0 = 1$ and $N_s = 8$. For the Wilson kernel we then have $\lambda_{\mathrm{min}} = 1$ and $\lambda_{\mathrm{max}} = 3$, for the staggered Wilson kernel $\lambda_{\mathrm{min}} = 1$ and $\lambda_{\mathrm{max}} = \sqrt{2}$. The corresponding example weights $\{\omega_s\}$ for optimal domain wall fermions can be found in Table II.

TABLE II. ω_s for optimal domain wall fermions.

s	$\omega_s(\lambda_{\mathrm{min}} = 1, \lambda_{\mathrm{max}} = 3)$	$\omega_s(\lambda_{\mathrm{min}} = 1, \lambda_{\mathrm{max}} = \sqrt{2})$
1	0.989011284192743	0.996659816028010
2	0.908522120246430	0.971110743060917
3	0.779520722603956	0.925723982088869
4	0.641124364053574	0.869740043520870
5	0.519919928211430	0.813009342796322
6	0.427613177773962	0.763841917102527
7	0.366896221792507	0.728142270322088
8	0.337036936444470	0.709476563432225

[1] R. Narayanan and H. Neuberger, Infinitely many regulator fields for chiral fermions, Phys. Lett. B **302**, 62–69 (1993).
[2] R. Narayanan and H. Neuberger, Chiral fermions on the lattice, Phys. Rev. Lett. **71**, 3251 (1993).
[3] R. Narayanan and H. Neuberger, Chiral determinant as an overlap of two vacua, Nucl. Phys. **B412**, 574 (1994).
[4] R. Narayanan and H. Neuberger, A construction of lattice chiral gauge theories, Nucl. Phys. **B443**, 305 (1995).
[5] H. Neuberger, Exactly massless quarks on the lattice, Phys. Lett. B **417**, 141 (1998).
[6] H. Neuberger, A Practical Implementation of the Overlap Dirac Operator, Phys. Rev. Lett. **81**, 4060 (1998).
[7] H. Neuberger, More about exactly massless quarks on the lattice, Phys. Lett. B **427**, 353 (1998).
[8] P. H. Ginsparg and K. G. Wilson, A remnant of chiral symmetry on the lattice, Phys. Rev. D **25**, 2649 (1982).

[9] P. Hasenfratz, V. Laliena, and F. Niedermayer, The index theorem in QCD with a finite cutoff, Phys. Lett. B **427**, 125 (1998).
[10] M. Luscher, Exact chiral symmetry on the lattice and the Ginsparg-Wilson relation, Phys. Lett. B **428**, 342 (1998).
[11] H. B. Nielsen and M. Ninomiya, Absence of neutrinos on a lattice: (I). Proof by homotopy theory, Nucl. Phys. **B185**, 20 (1981); **B195**, 541(E) (1982).
[12] H. B. Nielsen and M. Ninomiya, No Go theorem for regularizing chiral fermions, Phys. Lett. B **105**, 219 (1981).
[13] H. B. Nielsen and M. Ninomiya, Absence of neutrinos on a lattice: (II). Intuitive topological proof, Nucl. Phys. **B193**, 173 (1981).
[14] D. Friedan, A proof of the Nielsen-Ninomiya theorem, Commun. Math. Phys. **85**, 481 (1982).
[15] G. I. Egri, Z. Fodor, S. D. Katz, and K. K. Szabo, Topology with dynamical overlap fermions, J. High Energy Phys. 01 (2006) 049.
[16] H. Fukaya, S. Hashimoto, K.-I. Ishikawa, T. Kaneko, H. Matsufuru, T. Onogi, and N. Yamada (JLQCD Collaboration), Lattice gauge action suppressing near-zero modes of H_W, Phys. Rev. D **74**, 094505 (2006).
[17] N. Cundy, S. Krieg, T. Lippert, and A. Schafer, Topological tunneling with dynamical overlap fermions, Comput. Phys. Commun. **180**, 201 (2009).
[18] N. Cundy and W. Lee, Modifying the molecular dynamics action to increase topological tunnelling rate for dynamical overlap fermions, arXiv:1110.1948.
[19] D. B. Kaplan, A method for simulating chiral fermions on the lattice, Phys. Lett. B **288**, 342 (1992).
[20] Y. Shamir, Chiral fermions from lattice boundaries, Nucl. Phys. **B406**, 90 (1993).
[21] V. Furman and Y. Shamir, Axial symmetries in lattice QCD with Kaplan fermions, Nucl. Phys. **B439**, 54 (1995).
[22] P. M. Vranas, Chiral symmetry restoration in the Schwinger model with domain wall fermions, Phys. Rev. D **57**, 1415 (1998).
[23] S. Aoki and Y. Taniguchi, One loop calculation in lattice QCD with domain wall quarks, Phys. Rev. D **59**, 054510 (1999).
[24] Y. Kikukawa, H. Neuberger, and A. Yamada, Exponential suppression of radiatively induced mass in the truncated overlap, Nucl. Phys. **B526**, 572 (1998).
[25] P. Chen, N. H. Christ, G. T. Fleming, A. Kaehler, C. Malureanu, R. Mawhinney, G. Siegert, C. z. Sui, Y. Zhestkov, and P. M. Vranas, Toward the chiral limit of QCD: Quenched and dynamical domain wall fermions, in *High-energy physics. Proceedings, 29th International Conference, ICHEP'98, Vancouver, Canada, July 23-29, 1998. Vol. 1, 2* (1998).
[26] T. Blum, Domain wall fermions in vector gauge theories, in Lattice Field Theory. Proceedings: 16th International Symposium, Lattice '98, Boulder, USA, Jul 13-18, 1998, *Nucl. Phys. Proc. Suppl.* 73, 167 (1999).
[27] G. T. Fleming, How well do domain wall fermions realize chiral symmetry?, in Lattice field theory. Proceedings, 17th International Symposium, Lattice'99, Pisa, Italy, June 29-July 3, 1999, *Nucl. Phys. Proc. Suppl.* 83, 363 (2000).
[28] P. Hernandez, K. Jansen, and M. Luscher, A Note on the practical feasibility of domain wall fermions, in Workshop on Current Theoretical Problems in Lattice Field Theory Ringberg, Germany, April 2-8, 2000 (2000), arXiv:hep-lat/0007015.
[29] S. Aoki, T. Izubuchi, Y. Kuramashi, and Y. Taniguchi, Domain wall fermions in quenched lattice QCD, Phys. Rev. D **62**, 094502 (2000).
[30] K. G. Wilson, Quarks and strings on a lattice, in *New Phenomena In Subnuclear Physics. Part A. Proceedings of the First Half of the 1975 International School of Subnuclear Physics, Erice, Sicily, July 11–August 1, 1975*, edited by A. Zichichi (Plenum Press, New York, 1977), p. 69.
[31] D. H. Adams, Theoretical Foundation for the Index Theorem on the Lattice with Staggered Fermions, Phys. Rev. Lett. **104**, 141602 (2010).
[32] D. H. Adams, Pairs of chiral quarks on the lattice from staggered fermions, Phys. Lett. B **699**, 394 (2011).
[33] J. B. Kogut and L. Susskind, Hamiltonian formulation of Wilson's lattice gauge theories, Phys. Rev. D **11**, 395 (1975).
[34] T. Banks, L. Susskind, and J. B. Kogut, Strong coupling calculations of lattice gauge theories: $(1 + 1)$-dimensional exercises, Phys. Rev. D **13**, 1043 (1976).
[35] T. Banks, S. Raby, L. Susskind, J. Kogut, D. R. T. Jones, P. N. Scharbach, and D. K. Sinclair (Cornell-Oxford-Tel Aviv-Yeshiva Collaboration), Strong coupling calculations of the hadron spectrum of quantum chromodynamics, Phys. Rev. D **15**, 1111 (1977).
[36] L. Susskind, Lattice fermions, Phys. Rev. D **16**, 3031 (1977).
[37] M. F. L. Golterman and J. Smit, Self-energy and flavor interpretation of staggered fermions, Nucl. Phys. **B245**, 61 (1984).
[38] C. Hoelbling, Single flavor staggered fermions, Phys. Lett. B **696**, 422 (2011).
[39] S. R. Sharpe, Comments on non-degenerate staggered fermions, staggered Wilson and Overlap fermions, and the application of chiral perturbation theory to lattice fermions (2012).
[40] P. de Forcrand, A. Kurkela, and M. Panero, *Proc. Sci.* LATTICE2010 (2010) 080 [arXiv:1102.1000].
[41] P. de Forcrand, A. Kurkela, and M. Panero, Numerical properties of staggered quarks with a taste-dependent mass term, J. High Energy Phys. 04 (2012) 142.
[42] S. Durr, Taste-split staggered actions: eigenvalues, chiralities and Symanzik improvement, Phys. Rev. D **87**, 114501 (2013).
[43] D. H. Adams, D. Nogradi, A. Petrashyk, and C. Zielinski, *Proc. Sci.* LATTICE2014 (2014) 353 [arXiv:1312.3265].
[44] J. S. Schwinger, Gauge invariance and mass. II, Phys. Rev. **128**, 2425 (1962).
[45] A. M Tsvelik, *Quantum field theory in condensed matter physics* (Cambridge University Press, Cambridge, England, 2007).
[46] K. G. Wilson, Confinement of quarks, Phys. Rev. D **10**, 2445 (1974).
[47] Note that not all of the possible combinations of mass terms in Eq. (32) are practically useful.

[48] A. Borici, Truncated overlap fermions, in Lattice field theory. Proceedings, 17th International Symposium, Lattice'99, Pisa, Italy, June 29-July 3, 1999, Nucl. Phys. B, Proc. Suppl. **83**, 771 (2000).
[49] R. C. Brower, H. Neff, and K. Orginos, Möbius fermions: Improved domain wall chiral fermions, Lattice field theory. Proceedings, 22nd International Symposium, Lattice 2004, Batavia, USA, June 21-26, 2004, Nucl. Phys. B, Proc. Suppl. **140**, 686 (2005).
[50] N. J Higham, The matrix sign decomposition and its relation to the polar decomposition, in Linear Algebra Appl. **212**, 3 (1994).
[51] T.-W. Chiu, Optimal Domain Wall Fermions, Phys. Rev. Lett. **90**, 071601 (2003).
[52] T.-W. Chiu, Locality of optimal lattice domain wall fermions, Phys. Lett. B **552**, 97 (2003).
[53] E. I. Zolotarev, Application of elliptic functions to questions of functions deviating least and most from zero, Zap. Imp. Akad. Nauk. St. Petersburg **30**, 1 (1877); Reprinted in his Collected Works, Izdat. Akad. Nauk SSSR **II**, 1 (1932). In Russian.
[54] N. I. Akhiezer, *Elements of the Theory of Elliptic Functions*, Vol. 79 (American Mathematical Society, Washington, DC, 1990).
[55] N. I Achieser, *Theory of Approximation* (Courier Corporation, Chicago, 2013).
[56] J. van den Eshof, A. Frommer, T. Lippert, K. Schilling, and H. A. van der Vorst, Numerical methods for the QCD overlap operator. I. Sign function and error bounds, in Comput. Phys. Commun. **146**, 203 (2002).
[57] T.-W. Chiu, T.-H. Hsieh, C.-H. Huang, and T.-R. Huang, A note on the Zolotarev optimal rational approximation for the overlap Dirac operator, Phys. Rev. D **66**, 114502 (2002).
[58] M. Abramowitz and I. A. Stegun, *Handbook of Mathematical Functions: with Formulas, Graphs, and Mathematical Tables*, Dover Books on Mathematics (Dover, New York, 2012).
[59] Y.-C. Chen, T.-W. Chiu, T.-S. Guu, T.-H. Hsieh, C.-H. Huang, and Y.-Y. Mao (TWQCD Collaboration), *Proc. Sci.* LATTICE2010 (2010) 099 [arXiv:1101.0405].
[60] T.-H. Hsieh, T.-W. Chiu, and Y.-Y. Mao (TWQCD Collaboration), *Proc. Sci.* LATTICE2010 (2010) 085 [arXiv:1101.0402].
[61] T. W. Chiu, T. H. Hsieh, and Y. Y. Mao (TWQCD Collaboration), Topological susceptibility in two flavors lattice QCD with the optimal domain-wall fermion, Phys. Lett. B **702**, 131 (2011).
[62] T.-W. Chiu, T.-H. Hsieh, and Y.-Y. Mao (TWQCD Collaboration), Pseudoscalar meson in two flavors QCD with the optimal domain-wall fermion, Phys. Lett. B **717**, 420 (2012).
[63] Y.-C. Chen and T.-W. Chiu (TWQCD Collaboration), Chiral symmetry and the residual mass in lattice QCD with the optimal domain-wall fermion, Phys. Rev. D **86**, 094508 (2012).
[64] T.-W. Chiu and T.-H. Hsieh (TWQCD Collaboration), *Proc. Sci.* LATTICE (2012) 205.
[65] T.-W. Chiu, Domain-wall fermion with R_5 symmetry, Phys. Lett. B **744**, 95 (2015).
[66] R. C. Brower, H. Neff, and K. Orginos, Möbius fermions, in Hadron physics, Proceedings of the Workshop on Computational Hadron Physics, University of Cyprus, Nicosia, Cyprus, 2005, *Nucl. Phys. Proc. Suppl.* 153, 191–198 (2006).
[67] R. Brower, R. Babich, K. Orginos, C. Rebbi, D. Schaich, and P. Vranas, *Proc. Sci.* LATTICE2008 (2008) 034 [arXiv:0906.2813].
[68] H. Neuberger, Vectorlike gauge theories with almost massless fermions on the lattice, Phys. Rev. D **57**, 5417 (1998).
[69] Y. Kikukawa, Low-energy effective action of domain wall fermion and the Ginsparg-Wilson relation, Nucl. Phys. B, Proc. Suppl. **83**, 630 (2000).
[70] Y. Kikukawa, Locality bound for effective four-dimensional action of domain wall fermion, Nucl. Phys. **B584**, 511 (2000).
[71] Y. Shamir, Reducing chiral symmetry violations in lattice QCD with domain wall fermions, Phys. Rev. D **59**, 054506 (1999).
[72] Robert G. Edwards and Urs M. Heller, Domain wall fermions with exact chiral symmetry, Phys. Rev. D **63**, 094505 (2001).
[73] P. Boyle, A. Juttner, M. K. Marinkovic, F. Sanfilippo, M. Spraggs, and J. T. Tsang, An exploratory study of heavy domain wall fermions on the lattice, J. High Energy Phys. 04 (2016) 037.
[74] S. Durr, C. Hoelbling, and U. Wenger, Filtered overlap: Speedup, locality, kernel non-normality and $Z_A \simeq 1$, J. High Energy Phys. 09 (2005) 030.
[75] Maarten Golterman and Yigal Shamir, Localization in lattice QCD, Phys. Rev. D **68**, 074501 (2003).
[76] M. Golterman and Y. Shamir, Localization in lattice QCD (with emphasis on practical implications), in Lattice field theory. Proceedings, 21st International Symposium, Lattice 2003, Tsukuba, Japan, July 15-19, 2003, Nucl. Phys. B, Proc. Suppl. **129**, 149 (2004).
[77] M. Golterman, Y. Shamir, and B. Svetitsky, Mobility edge in lattice QCD, Phys. Rev. D **71**, 071502 (2005).
[78] M. Golterman, Y. Shamir, and B. Svetitsky, Localization properties of lattice fermions with plaquette and improved gauge actions, Phys. Rev. D **72**, 034501 (2005).
[79] T. Blum, P. Chen, N. Christ, C. Cristian, C. Dawson, G. Fleming, A. Kaehler, X. Liao, G. Liu, C. Malureanu, R. Mawhinney, S. Ohta, G. Siegert, A. Soni, C. Sui, P. Vranas, M. Wingate, L. Wu, and Y. Zhestkov, Quenched lattice QCD with domain wall fermions and the chiral limit, Phys. Rev. **D69**, 074502 (2004).
[80] T. Blum, N. Christ, C. Cristian, C. Dawson, G. Fleming, G. Liu, R. Mawhinney, A. Soni, P. Vranas, M. Wingate, L. Wu, and Y. Zhestkov, Nonperturbative renormalization of domain wall fermions: Quark bilinears, Phys. Rev. D **66**, 014504 (2002).
[81] V. Gadiyak, X.-D. Ji, and C.-W. Jung, Domain wall induced quark masses in topologically nontrivial background, Phys. Rev. D **62**, 074508 (2000).
[82] C. Jung, R. G. Edwards, X.-D. Ji, and V. Gadiyak, Residual chiral symmetry breaking in domain wall fermions, Phys. Rev. D **63**, 054509 (2001).

[83] C. Jung, R. G. Edwards, X.-D. Ji, and V. Gadiyak, Residual chiral symmetry breaking in domain wall fermions, in Lattice field theory. Proceedings, 18th International Symposium, Lattice 2000, Bangalore, India, August 17-22, 2000, Nucl. Phys. B, Proc. Suppl. **94**, 748–751 (2001).
[84] M. F. Atiyah and I. M. Singer, The index of elliptic operators: I, Ann. Math. **87**, 484 (1968).
[85] M. F. Atiyah and I. M. Singer, The index of elliptic operators: III, Ann. Math. **87**, 546 (1968).
[86] M. F. Atiyah and I. M. Singer, The index of elliptic operators: IV, Ann. Math. **93**, 119 (1971).
[87] M. F. Atiyah and I. M. Singer, The index of elliptic operators: V, Ann. Math. **93**, 139 (1971).
[88] J. E. Kiskis, Fermions in a pseudoparticle field, Phys. Rev. D **15**, 2329 (1977).
[89] N. K. Nielsen and B. Schroer, Axial anomaly and Atiyah-Singer theorem, Nucl. Phys. **B127**, 493 (1977).
[90] M. M. Ansourian, Index theory and the axial current anomaly in two-dimensions, Phys. Lett. B **70**, 301 (1977).
[91] W. Kerler, Dirac operator normality and chiral fermions, Chin. J. Phys. (Taipei) **38**, 623 (2000).
[92] I. Hip, T. Lippert, H. Neff, K. Schilling, and W. Schroers, Instanton dominance of topological charge fluctuations in QCD?, Phys. Rev. D **65**, 014506 (2001).
[93] I. Hip, T. Lippert, H. Neff, K. Schilling, and W. Schroers, The Consequences of non-normality, in Contents of Lattice 2001 Proceedings, Nucl. Phys. B, Proc. Suppl. **106**, 1004 (2002).
[94] S. Durr and G. Koutsou, Brillouin improvement for Wilson fermions, Phys. Rev. D **83**, 114512 (2011).
[95] D. H. Adams, R. Har, Y. Jia, and C. Zielinski, *Proc. Sci.* LATTICE2014 (2014) 462 [arXiv:1312.7230].
[96] V. Azcoiti, G. Di Carlo, E. Follana, and A. Vaquero, Topological index theorem on the lattice through the spectral flow of staggered fermions, Phys. Lett. B **744**, 303 (2015).
[97] J. Smit and J. C. Vink, Remnants of the index theorem on the lattice, Nucl. Phys. **B286**, 485 (1987).
[98] R. B. Lehoucq, D. C. Sorensen, and C. Yang, *ARPACK Users Guide: Solution of Large Scale Eigenvalue Problems by Implicitly Restarted Arnoldi Methods* (Society for Industrial and Applied Mathematics, Philadelphia, 1997).
[99] E. Anderson, Z. Bai, C. Bischof, S. Blackford, J. Demmel, J. Dongarra, J. Du Croz, A. Greenbaum, S. Hammarling, A. McKenney, and D. Sorensen, *LAPACK Users' Guide*, 3rd ed. (Society for Industrial and Applied Mathematics, Philadelphia, 1999).
[100] S. Durr and C. Hoelbling, Staggered versus overlap fermions: A study in the Schwinger model with $N_f = 0$, 1, 2, Phys. Rev. D **69**, 034503 (2004).
[101] S. Durr and C. Hoelbling, Scaling tests with dynamical overlap and rooted staggered fermions, Phys. Rev. D **71**, 054501 (2005).
[102] L. Giusti, C. Hoelbling, and C. Rebbi, Schwinger model with the overlap Dirac operator: Exact results versus a physics motivated approximation, Phys. Rev. D **64**, 054501 (2001).
[103] S. Durr and C. Hoelbling, Lattice fermions with complex mass, Phys. Rev. D **74**, 014513 (2006).
[104] M. Falcioni, M. L. Paciello, G. Parisi, and B. Taglienti, Again on SU(3) glueball mass, Nucl. Phys. **B251**, 624 (1985).
[105] M. Albanese*et al.*, (APE Collaboration), Glueball masses and string tension in lattice QCD, Phys. Lett. B **192**, 163 (1987).
[106] S. Capitani, S. Durr, and C. Hoelbling, Rationale for UV-filtered clover fermions, J. High Energy Phys. 11 (2006) 028.
[107] S. Itoh, Y. Iwasaki, and T. Yoshie, The U(1) problem and topological excitations on a lattice, Phys. Rev. D **36**, 527 (1987).
[108] E. Follana, V. Azcoiti, G. Di Carlo, and A. Vaquero, *Proc. Sci.* LATTICE2011 (2011) 100 [arXiv:1111.3502].